A GTO-BASED THREE-PHASE AC-DC PWM CONVERTER FED DC MOTOR

By

JAMAL JAFAR JAFAR

DEPARTMENT OF ELECTRICAL ENGINEERING

INDIAN INSTITUTE OF TECHNOLOGY KANPUR

JULY, 1995

A GTO-BASED THREE-PHASE AC-DC PWM CONVERTER FED DC MOTOR

A Thesis Submitted in Partial Fulfilment of
Requirements for the Degree of

Master of Technology

By

JAMAL JAFAR JAFAR

TO THE

DEPARTMENT OF ELECTRICAL ENGINEERING
INDIAN INSTITUTE OF TECHNOLOGY KANPUR

JULY 1995

EE-1995-M-JAF-GTO

TO

ALZAHRAA

CERTIFICATE

It is certified that the work contained in the thesis entitled "A GTO-BASED THREE-PHASE AC-DC PWM CONVERTER FED DC MOTOR" by Jamal Jafar (Roll No. 9320401), has been carried out under my supervision and this work has not been submitted else where for a degree.

Date : 7/7/1995

Dr. B.G. Fernandes
Assistant Professor
Department of Electrical Engineering
Indian Institute of Technology
Kanpur - 208016

ACKNOWLEDGEMENTS

I wish to record my deep sense of gratitude to Dr. B.G. Fernandes for his most valuable guidance and encouragement throughout the course of this project work. My thanks are due to faculty members of E.E. Department, particularly Dr. M.U. Siddiqi (Head, EE/ACES), Dr. G.K. Dubey, Dr. S.S. Prabhu, Dr. S.C. Srivastava, Dr. A. Joshi, Dr. R. Arora, Dr. M.M. Hassan, Dr. B. Mazhari.

I gratefully acknowledge the help and co-operation of the staff of P.E. Lab., workshop, and store. I am indeed thankful to Aleppo University for having sopnsored me and I.I.T. Kanpur for having provided me the facilities to carry out this work.

I am grateful to my friends and colleagues especially Kishore Chatterjee and Sheshu Kumar from whom I am greatly benefitted through discussions and with whom working was a pleasure.

.Finally, I thank my wife and my daughter ALZAHRAA for their understanding and patience, which made this work possible. I thank Mr. Ajai Kumar Srivastava for the excellent job done in typing this thesis.

Jamal Jafar

CONTENTS

LIST OF FIGURES

LIST OF OSCILLOGRAMS

LIST OF SYMBOLS

	Gate Turn-Off Thyristor
	Pulse-Width Modulation
1	Programmed PWM technique
e_B, e_C	Line to neutral voltage of a three-phase Ac source, V
, e_{BC}, e_{CA}	Line to Line voltage of a three-phase Ac source, V
	RMS voltage per phase of a three-phase Ac source, V
	Angular frequency of Ac source, rad/sec.
β_i	Firing and extinction angles for i^{th} pulse per cycle, rad.
	Instantaneous armature voltage, V
	Instantaneous armature current, A
	Average value of v_a, V
ax	Maximum average voltage for six pulses converter, V
	Total number of output voltage pulses per cycle
	Phase angle difference between e_A and the line voltage used to produce i^{th} pulse, rad.
	The number of pulses per half cycle
b_n	The fourier co-efficients
	Amplitude of the fundamental wave
	Armature circuit resistance, ohms
	Armature circuit inductance, henery
	Armature circuit impedance, ohms
	Quality factor of armature circuit
	Motor back emf under steady state, V
$_{bn}$	Normalized values of i_a and E_b respectively
	Source current in phase A, A
	Control voltage, V
R_f	RC elements connected across source terminals, ohms, μFarads
L_S	Source internal resistance and inductance, ohms, henery
2	Resistor used for measureing input current & output current, ohms, ohms
	Resistive load for dc generator

ABSTRACT

The present work deals with designing of three-phase GTO AC-DC converter and its control circuit, snubber circuit and drive circuit. The GTO thyristors are switched employing programmed PWM technique to eliminate some lower order harmonics. The analysis of converter circuit is presented.Digital technique is used to implement the above PWM technique.The system is tested experimentally to verify the basic principles and analytical results.

CHAPTER I

INTRODUCTION

General :

Thyristorised power controllers are now widely used in the industry. Conventional controllers have been replaced by thyristorised power controllers in almost all applications. The prominent applications of such controllers [1], are as follows :

1. Control of ac and dc drives in rolling mills, paper and textile mills, traction vehicles, mine winders .....etc.

2. Uninterruptible and standby power supplies for critical loads (air craft and space applications)

3. Power control in metallurgical and chemical processes.

4. Static power compensators and static conductors.

5. HVDC transmission System.

6. HV supplies for electrostatic precipitators and X-ray generators.

7. Illumination control for lighting.

8. Solid state controllers for home appliances.

Some of the important advantages associated with thyristorised power controllers are:

1. High efficiency.
2. Long Life and reduces maintenance.
3. Compact size, low weight, volume and noise.
4. Flexibility in operation due to digital controls.
5. Fast dynamic response.
6. Better reliability and high quality performance.

DC drives are widely used in applications requiring adjustable speed, good speed regulation and frequent starting, braking and reversing. In comparison with ac drives they offer several advantages such as low overall cost, simple control circuitry, and versatile control characteristics.

The speed control of DC motors is often achieved by controlled rectification of ac supply by means of thyristor bridge. The controlled rectification provides smooth variation of motor speed and regenerative braking of the drive. Phase controlled rectifiers are widely used for controlled rectification because these converters are simple, less expensive, reliable and do not require special commutation schemes for the thyristors.

But, the supply power factor in phase controlled converter decreases with the triggering angle. The displacement angle between the supply voltage and the supply current increases with triggering angle. Hence, the reactive power drawn by the converter increase, thereby decreasing the power factor. The reactive power drawn from the line, when operating at low power

factor, increases the transmission losses and maximum power demand and has adverse effect on voltage regulation and supply system stability.

The phase controlled converter also introduces ripple in the load current and harmonics in the source current. This ripple current increases the copper losses and lowers the efficiency of the drive system. It may cause the derating of the motor and may affect the machine commutation.

The source current harmonics have a number of undesirable effects [2], such as :

- reduces the overall power factor
- causes the radio frequency interface (noice interface with communication line).
- malfunction of electronic equipments connected to the line.
- overloading of capacitors, generators and inductors.
- decrease in efficiency owing to increase in losses due to harmonic current and skin effect.
- Saturation of transformers.

Therefore, alternative control schemes which overcome these drawbacks and provide smooth variation of output voltage are highly desirable. A number of techniques have been developed to improve the performance of the converter, keeping in view the input power factor, source current harmonics, system efficiency, load current ripple, complexity of control

circuit and the cost of the drive. Some of them are :

increasing the converter pulse number :

The system performance can be improved by increasing the number of phases in the ac supply. But, this involves high cost in terms of additional thyristors and control circuits.

using fully controlled converter with half Controlled characteristics :

The advantages of half controlled converter are counter-balanced by the fact that its operations is confined to single quadrant.

sequence control technique :

Another method of improving system performance is to connect two or more stages of single phase converter bridge, in series and operate by sequence control technique. Such arrangements, though expensive, are widely used in medium power traction applications where the power factor becomes an imperative necessity.

McMurrcy [3], Mukhopadhyaya [4], Stefanovic [5] and Ohnishi et al [6] proposed a converter circuit configuration with phase controlled to improve supply power factor.

However, all the techniques mentioned above employ phase delay control for the variation of the output voltage, and they offer only a marginal improvement in the performance. However,

a significant improvement in both load side and source side performances is obtained by making use of forced commutation technique.

There are many techniques based on forced commutation which make the displacement factor (the fundamental power factor) unity and is independent of the magnitude of the output voltage. It is possible to keep the displacement factor at unity if the supply voltage is switched symmetrically with respect to the peak of the supply voltage. Such a control technique is termed as pulse-width modulation (PWM). The ripple in the output current and lower order harmonics in the source current are reduced considerably by producing multiple voltage pulses at the output. By doing this the higher order harmonics in the source current are increased, they can be filtered out easily by using a small LC filter at the source terminals.

Pulse-width modulated ac-dc thyristor converters have been suggested to improve the performance of the line commutated ac-dc converters. With this, there is a significant improvement of input power factor, distortion of the line current and the ripple in the output current. But, these converters use very bulky commutation circuits for forced commutation. This results in considerable increase in losses, weight, volume and the cost of forced commutated converters. But, the recent advances in power semiconductor technology has led to the development of self commutated switches like :

- Bipolar Junction Transistor, (BJT)
- Metal-Oxide-Semiconductor Field Effect Transistor, (MOSFET)
- Insulated Gate Bipolar Transistor (IGBT) and
- Gate turn-off thyristor (GTO)

All these devices can be controlled by using appropriate voltage or current signals at the gate terminal. These devices do not require the forced commutation circuits, which results in considerable reduction in converter losses, volume, weight and cost. This make the converter more compact and reliable. Due to high switching speeds of the self-commutated devices, they can be operated at higher frequencies. Hence, the magnitude of lower order harmonics can be considerably reduced. However, due to lower voltage and current ratings of BJT, MOSFET & IGBT, the use of these devices is restricted to low power applications. GTO's are now commercially available upto 4500 volts and 4000 Amps. GTO with their higher voltage and current ratings are fast revolutionizing the PWM converter designs for large power applications. Because of this reason, GTO's have been used here as the self commutated switches in PWM ac-dc converter.

Performance characteristics of power conversion schemes largely depend on the choice of the practicular PWM strategy employed. PWM schems can be classified as :

(a) Carrier modulated wave PWM : Which includes :

(i) Equal pulse-width modulation (EPWM)

(ii) Triangular pulse-width modulation (TPWM)

(iii) Stepped pulse-width modulation (STPWM)

(iv) Sinusoidal pulse-width modulation (SPWM)

(v) Inverted sine pulse-width modulation (ISPWM)

(b) Precalculated programmed pulse width modulation (PPWM)

PPWM scheme exhibits several distinct advantages in comparison to carrier-modulated wave PWM scheme [7]. They are:

(1) About 50% reduction in the switching frequency. This results in reduction of switching losses.

(2) Harmonic interference such as resonace with the external filtering networks employed in the converter power supplies, is eliminated.

(3) The use of precalculated optimized PPWM switching patterns avoids on-line computations and provides straight forward implementation of a high-performance technique.

(4) Reduced ripple in the output current.

(5) Elimination of several lower order-harmonics generates high quality input spectra which in turn improves the performance.

Presently, enhancement in computing power and calculating procedures, the non-linear equations associated with selective elimination of harmonics can be easily solved. Also, with the availability of inexpensive large memories, these angles can be stored in EPROM. In view of this, PPWM technique hasemerged as an important and viable means of power control.

Organization of the Thesis :

The main motivation of this thesis can be described as developing a GTO-Based three-phase ac-dc converter with programmed PWM technique for dc motor drive.

A review of different configurations of power circuit and their control scheme which is reported in the literature is presented in chapter II. Chapter III deals with the open loop analysis of the drive system with PPWM technique.

Design and development of the hardware to implement the PPWM technique and control of the converter fed dc motor, are delt in chapter IV. All the design aspects of power circuit, gate drive circuit, snubber circuit and control circuit are also explained in this chapter.

Chapter V describes the detailed testing and performance evaluation of the converter fed dc motor drive. Chapter VI summarizes the conclusions of the work and gives suggestions for future work in this direction.

CHAPTER II

LITERATURE REVIEW

A brief review of the literature on three phase PWM ac-dc converters is presented in this chapter.

S.R. Doradla et al [8] and N.D. Prasad [9] have studied a three-phase ac-dc PWM converter controlled dc motor employing forced commutation. The converter shown in Fig. (2.1), contains three thyristers (SCR's) with forced commutation on upper limb of the bridge, while another three thyristers (SCR's) on the lower limb with line commutation. The forced commutated SCR's are gated many times in one ac cycle depending on the number of voltage pulses required at the output. The width of the output pulses is controlled in order to control the average output voltage. Though, the power factor is improved significantly, the converter requires an additional investment due to the passive elements required for forced commutation.

Inaba et al [10] have simplified the above mentioned converter circuit by replacing the forced commutated SCR's with GTO's. The power circuit configuration is shown in Fig. (2.2). Once the minimum pulse width is attained, its pulse position is shifted with respect to the source voltage, and the width of the pulse is maintained constant. This extends the control in the lower range of the ouput voltage, but the phase angle can not be extended upto 180^{o}. This is due to the fact that at this

extreme point, the line voltage polarities are not suitable for line commutation of SCR's in the lower limb.

Fig. (2.3) shows a six GTO ac-dc converter employing optimal PWM scheme. This configuration is proposed by Kataoka et al [11]. The over voltage which appears across source terminals when the line current is interrupted, is absorbed by capacitor, C through a diode bridge. The energy stored in C is dissipated in Resistor R. In this converter, the line current harmonics below the most predominant one are almost completely eliminated. But the number of switching operations are increased as compared to that of Equal Pulse-Width Modulation (EPWM) for the same number of output pulses per cycle. This converter requires a relatively complex control circuitry to implement the optimal PWM scheme. The variation of the output voltage is also limited in this converter configuration.

However, converters described in [10] and [11], the operation of the converter is limited to only one quadrant. The sequence of triggering pulses should be changed whenever the operation has to change from rectification to inversion mode or vice versa.

Viriya et al [12] have described a GTO-based ac-dc converter, which is shown in Fig. (2.4). This converter consists of two circuits, namely main circuit and auxiliary circuit. The main circuit consists of a three-phase bridge rectifier using six GTO's, and auxiliary circuit consists of

eight diodes , two GTO's, two inductors and a capacitor. The auxiliary circuit used to recover the commutating energy in the main circuit and to clamp the commutating impulse voltage at a desired level. PWM technique is used to trigger the main GTO's. They are controlled in a special sequence. This make the control circuit is more complex. Also since the auxiliary circuit requires extra elements, converter cost increases.

B.H. Khan in [13] has studied an PWM ac-dc GTO converter which consists of six GTO's. Here, the control circuit makes use of a combination of pulse width control and phase angle control to achieve continuous and smooth control of output voltage in two quadrants. The author has made comparative study of various carrier modulated wave PWM schemes (EPWM, SPWM, TPWM, STPWM, and ISPWM).

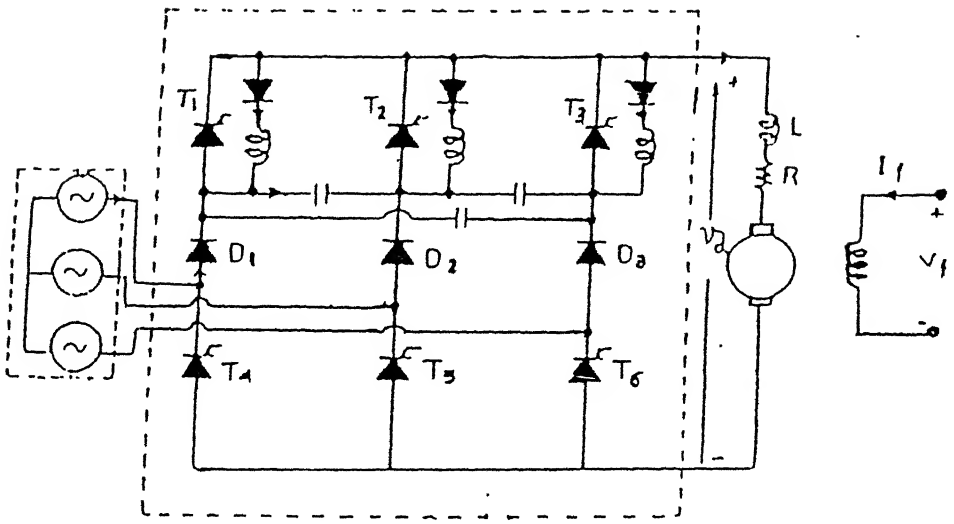

FIG. 2-1 CONVERTER PROPOSED BY DORADLA et al.

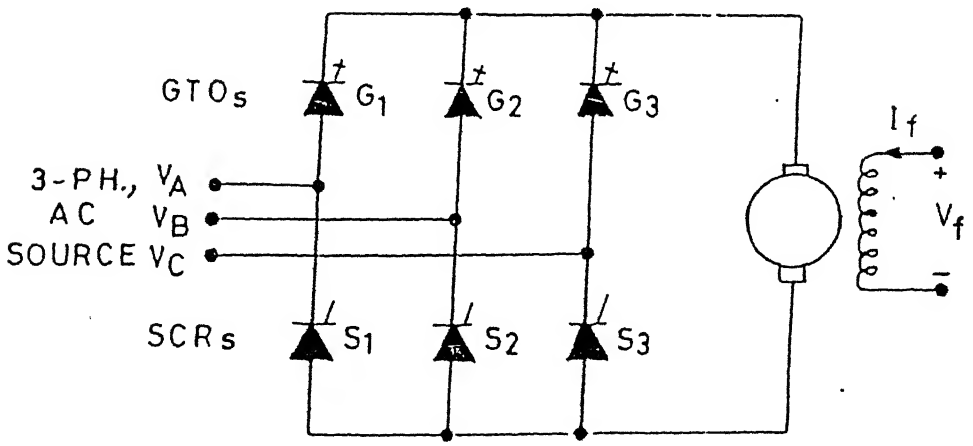

FIG. 2-2 CONVERTER PROPOSED BY INABA et al.

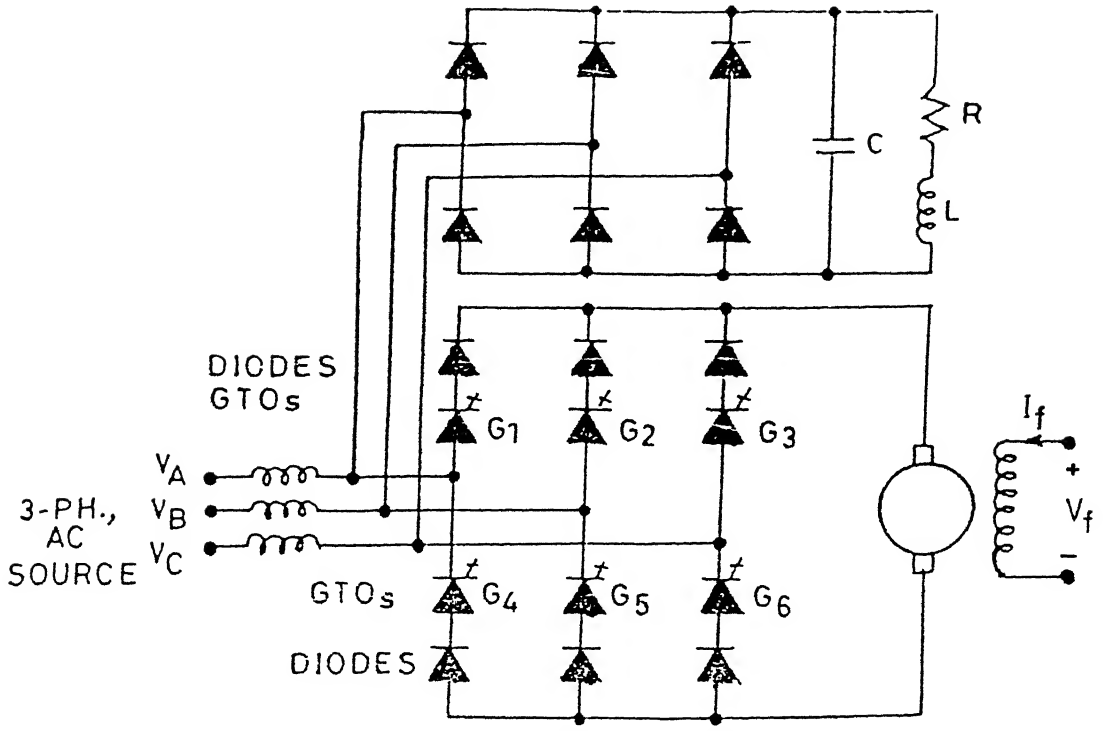

FIG. 2-3 CONVERTER PROPOSED BY KATAOKA et al.

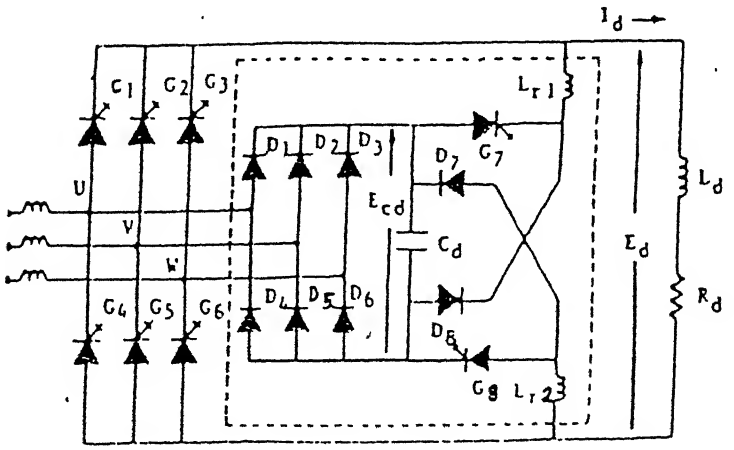

FIG. 2-4 CONVERTER PROPOSED BY VIRIYA et al.

CHAPTER III

ANALYSIS OF THREE-PHASE PWM AC-DC CONVERTER

Introduction :

PWM ac-dc converter has many advantages over phase controlled converter such as higher power factor, reduced ouput current ripple,reduced zone of discontinuous conduction, and reduced lower order harmonics in line current. However, forced commutation circuitry is to be provided with SCR's which increases the complexity of the converter.

Due to the progress in the semiconductor technology, high power self commutating devices are commercially available. So GTO's are now being used in high power applications. This results in simplified converter conifiguration due to the absence of commutating elements in the power circuit.

Analysis of three-phase PWM converter :

For the purpose of analysis a three-phase PWM ac-dc converter connected to a separately excited dc motor shown in Fig. (3.1) is considered. Where G_1- G_6 are self commutated switches (GTO's). Switching instants are determined by programmeed PWM technique. The system is analysed under the following assumptions :

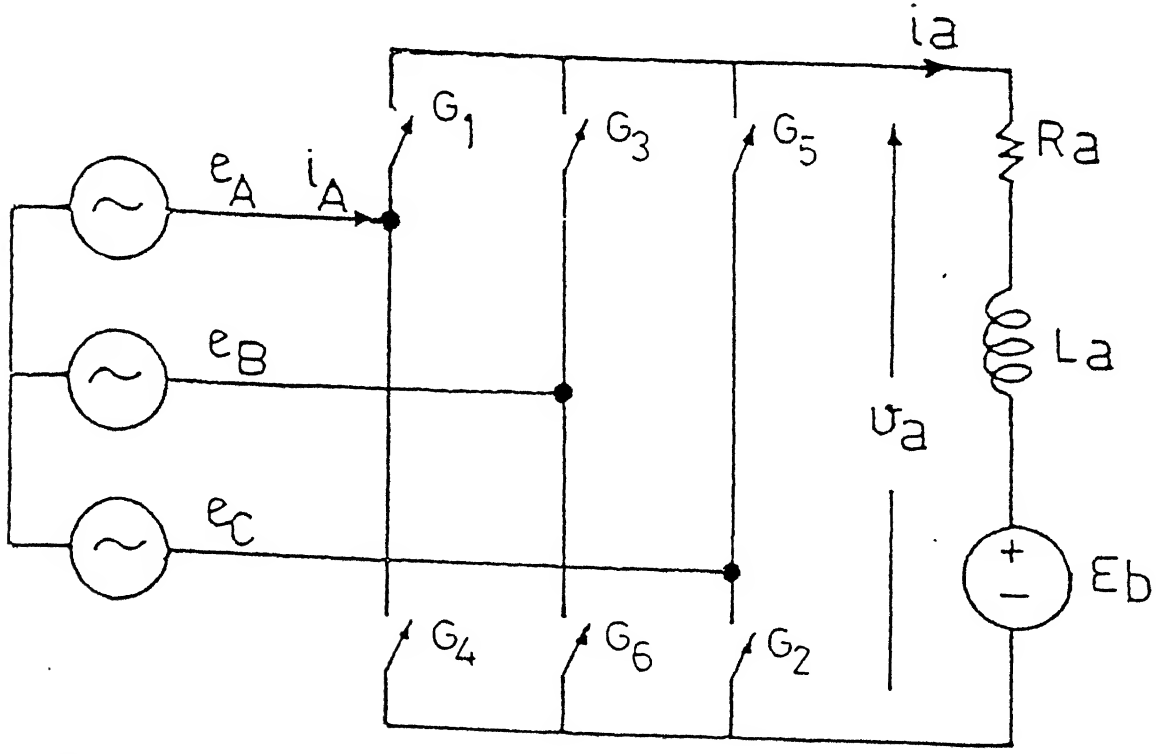

FIG. 3.1. IDEAL 3-PHASE PWM AC-DC CONVERTER.

(i) The power switches are ideal

(ii) The source is ideal, source impedance is zero.

(iii) Under steady state condition, the moter speed is constant.

(iv) The resistance and reactance of the dc motor remain constant throughout the operation.

The source voltage is expressed as :

$$e_A = \sqrt{2}\ V_{ph} \text{ Sin } (wt)$$

$$e_B = \sqrt{2}\ V_{ph} \text{ Sin } (wt - \frac{2\pi}{3})$$

$$e_C = \sqrt{2}\ V_{ph} \text{ Sin } (wt - \frac{4\pi}{3})$$

$$e_{AB} = e_A - e_B = \sqrt{6}\ V_{ph} \text{ Sin } (wt + \frac{\pi}{6})$$

$$e_{BC} = e_B - e_C = \sqrt{6}\ V_{ph} \text{ Sin } (wt - \frac{\pi}{2})$$

$$e_{CA} = e_C - e_A = \sqrt{6}\ V_{ph} \text{ Sin } (wt - \frac{7\pi}{6})$$

.1 The output Voltage :

The general waveform of output voltages v_a of the three-phase PWM ac-dc converter is shown in Fig. (3.2). Due to the three-phase symmetry, the average output voltage V_{av} is calculated by averaging v_a for a period $\frac{2\pi}{3}$,and expressed in terms of the maximum average voltage V_{avmax} of the six pulse converter. The expression of V_{av} and V_{avmax} are given by :

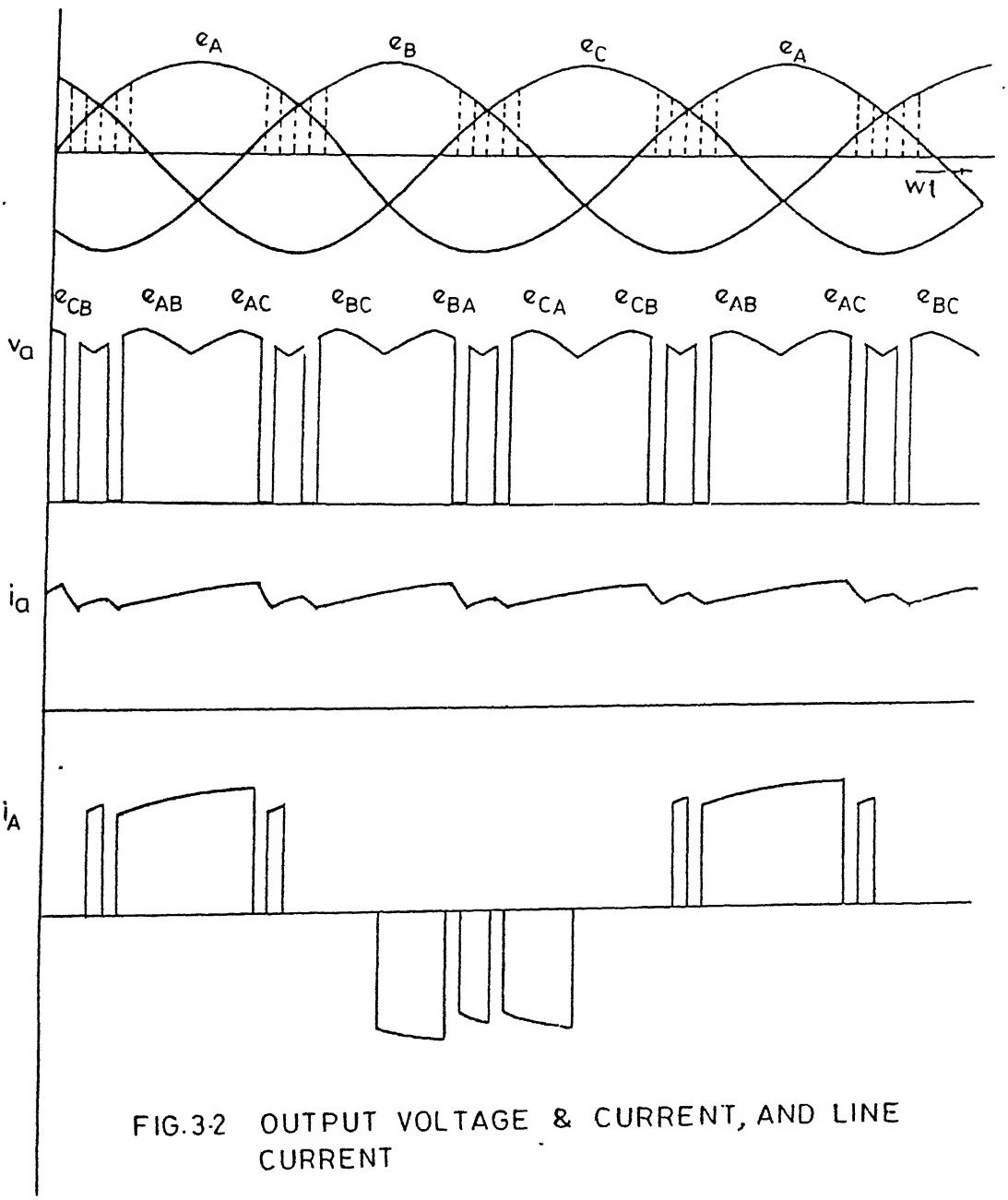

FIG. 3-2 OUTPUT VOLTAGE & CURRENT, AND LINE CURRENT

$$V_{av} = \frac{1}{2\pi/3}\sqrt{6}\ V_{ph} \sum_{i=1}^{p} \int_{\frac{\pi}{6}+\alpha_i}^{\frac{\pi}{6}+\beta_i} \text{Sin}\ (wt + \theta_r)\ d\ (wt)$$

$$V_{avmax} = \frac{3}{\pi}\sqrt{3}\ V_{ph}$$

$$V_{av} = V_{avmax} \sum_{i=1}^{p/2} \left[\text{Cos}\ (\frac{\pi}{3} + \alpha_i) - \text{Cos}\ (\frac{\pi}{3} + \beta_i) \right]$$

Where θ_r is the phase angle difference between e_A and the line voltage used to produce i^{th} pulse.

.2 The output current :

Fig. (3.2) shows the current waveform i_a, when a voltage v_a is applied across an R-L-E_b load. The expression for this current during i^{th} pulse can be written as :

$$i_a = \frac{\sqrt{6}\ V_{ph}}{Z_a}\ \text{Sin}\ (wt + \theta_r - \phi) - \frac{E_b}{R_a}$$

$$+ \left[I_{\alpha i} + \frac{E_b}{R_a} - \frac{\sqrt{6}\ V_{ph}}{Z_a}\ \text{Sin}\ (\alpha_i + \frac{\pi}{6} + \theta_r - \phi) \right] .$$

$$\exp\ (- \frac{wt - \alpha_i - \frac{\pi}{6}}{Q_1})$$

$$\text{for} \quad \frac{\pi}{6} + \alpha_i \leq wt \leq \frac{\pi}{6} + \beta_i$$

and,

$$i_a = \frac{-E_b}{R_a} + \left[I_{\beta i} + \frac{E_b}{R_a} \right] . \exp\ (- \frac{wt - \beta_i - \frac{\pi}{6}}{Q_1})$$

$$\text{for} \quad \frac{\pi}{6} + \beta_i \leq wt \leq \frac{\pi}{6} + \alpha_{i+1}$$

Where $Q_1 = \frac{wL_a}{R_a}$

$\phi = \tan^{-1} Q_1$

$I_{\alpha i}$: armature current at the beginning of the i^{th} pulse

$I_{\beta i}$: armature current at the end of the i^{th} pulse

$$Z_a = \sqrt{R_a^2 + (wL_a)^2}$$

Taking $\sqrt{6}\ V_{ph}$ as base voltage and, $\frac{\sqrt{6}\ V_{ph}}{Z_a}$ as base current

the expression for normalized current can be written as :

$$i_{an} = \text{Sin}\ (\ wt + \theta_r - \phi\ ) - \frac{E_{bn}}{\text{Cos}\ \phi} + \left[\ I_{\alpha in} + \frac{E_{bn}}{\text{Cos}\ \phi} - \text{Sin}\ (\ \alpha_i + \frac{\pi}{6} + \theta_r - \phi\ )\right] .\ \exp\ (\ -\ \frac{wt - \alpha_i - \frac{\pi}{6}}{Q_1}\ )$$

for $\quad \frac{\pi}{6} + \alpha_i \leq wt \leq \frac{\pi}{6} + \beta_i$

and,

$$i_{an} = -\ \frac{E_{bn}}{\text{Cos}\ \phi} + \left[\ I_{\beta in} + \frac{E_{bn}}{\text{Cos}\ \phi}\ \right] .\exp\ (\ -\ \frac{wt - \beta_i - \frac{\pi}{6}}{Q_1}\ )$$

for $\quad \frac{\pi}{6} + \beta_i \leq wt + \leq \frac{\pi}{6} + \alpha_{i+1}$

This expression is used to calculate the waveform of load current when the drive system is operating in motoring mode. During regenerating the polarity of back emf is reversed and firing/extinction angles are shifted by 180^{o}.

Harmonic Elimination technique for three phase converter :

Fig. (3.3) shows a general classification of PPWM techniques which eliminate harmonics and PPWM techniques with harmonic elimination suitable for three phase converter is shown in Fig. (3.4). The quarter wave symmetric three-phase line to line switching function employing positive, zero and negative switching states is shown in Fig. (3.5). The fourier co-efficients can be written as :

$$\left.\begin{aligned} a_n &= \frac{4}{n\pi}\left[\sum_{k=1}^{N}(-1)^{K+1}\,\mathrm{Cos}\,(n\,\alpha_k)\right] \\ b_n &= 0 \end{aligned}\right\} \quad \ldots\ldots\ldots (3.1)$$

Where,

$0 < \alpha_1 < \alpha_2 \ldots\ldots\ldots\ldots\ldots < \alpha_N < \frac{\pi}{3}$

N is a number of pulses per half cycle.

Switching angles α_{N+1} to α_{2N} are obtained by folding symmetry [14].

From equation (3.1), the non-linear equations for eliminating N-1 non-triplen harmonics such as 5, 7, 11, 13.....etc. are given by :

$$\left.\begin{aligned}
\alpha_1 - \cos\alpha_2 + \ldots\ldots\ldots\ldots + (-1)^{N+1}\cos\alpha_N &= \frac{\pi a_1}{4} \\
5\alpha_1 - \cos 5\alpha_2 + \ldots\ldots\ldots\ldots + (-1)^{N+1}\cos 5\alpha_N &= 0 \\
\cdot \qquad\qquad \cdot \qquad\qquad &\cdot \\
\cdot \qquad\qquad \cdot \qquad\qquad &\cdot \\
x\alpha_1 - \cos x\alpha_2 + \ldots\ldots\ldots\ldots + (-1)^{N+1}\cos x\alpha_N &= 0
\end{aligned}\right\} \qquad (3.2)$$

ere,

$x = 3N-1$ When N is even

$x = 3N-2$ When N is odd

e switching function is determined by solving the above n-linear equations for the first 60^0 interval of the input cle. The resulting equations to eliminate 5^{th} and 7^{th} rmonics are given by :

$N = 3 \qquad x = 7$

$$\left.\begin{aligned}
\cos\alpha_1 - \cos\alpha_2 + \cos\alpha_3 &= \frac{\pi a_1}{4} \\
\cos 5\alpha_1 - \cos 5\alpha_2 + \cos 5\alpha_3 &= 0 \\
\cos 7\alpha_1 - \cos 7\alpha_2 + \cos 7\alpha_3 &= 0
\end{aligned}\right\} \qquad (3.3)$$

e equations (3.3) are solved for α_1, α_2 and α_3. The amplitude fundamental wave a_1 in p.u was varied from 0.1 to 1.12 and for ch value, three commutation angles (α_1, α_2 and α_3) are termined. The set of angles are given in Appendix VI.

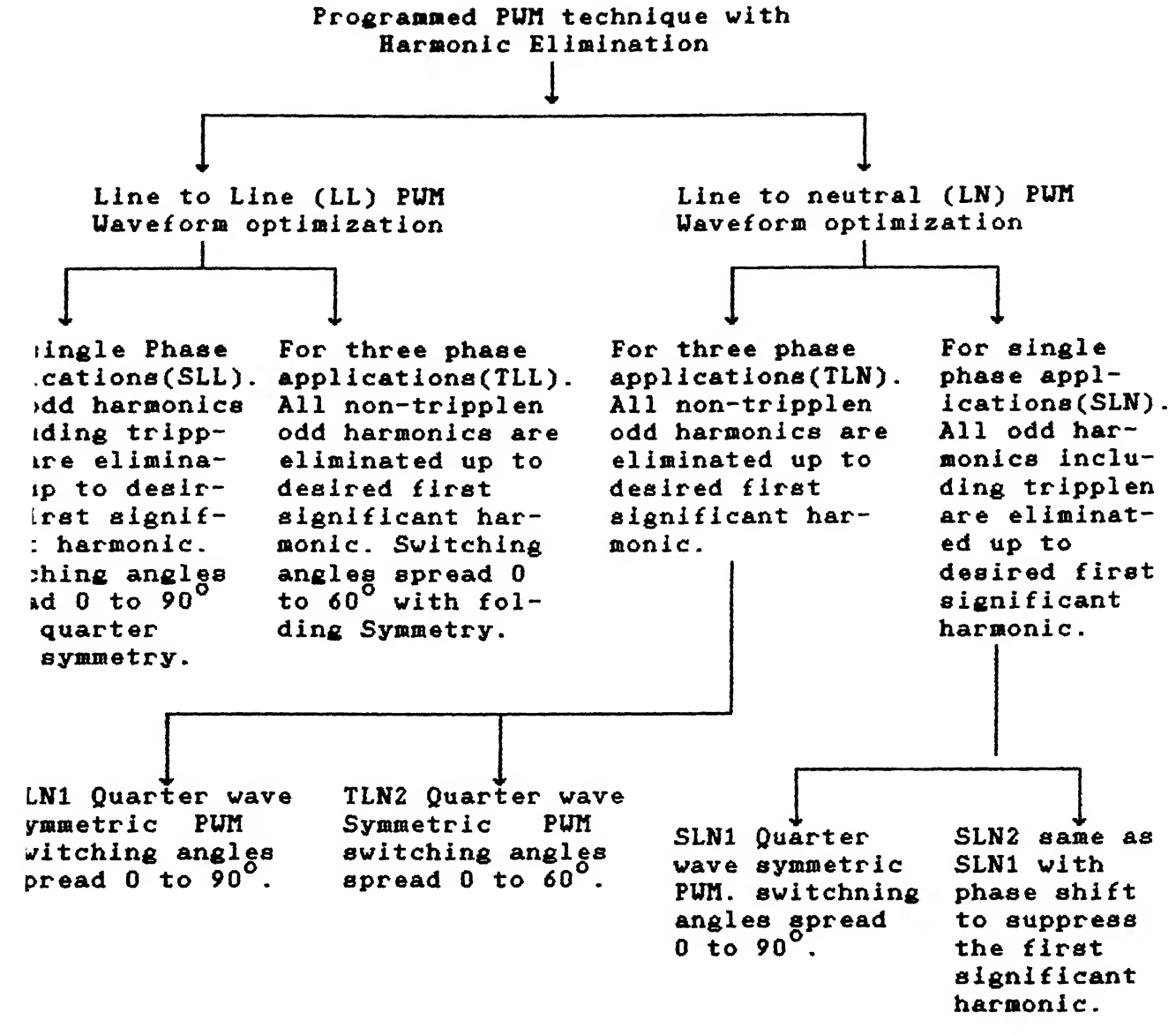

Fig. 3.3 General classification of programmed PWM's

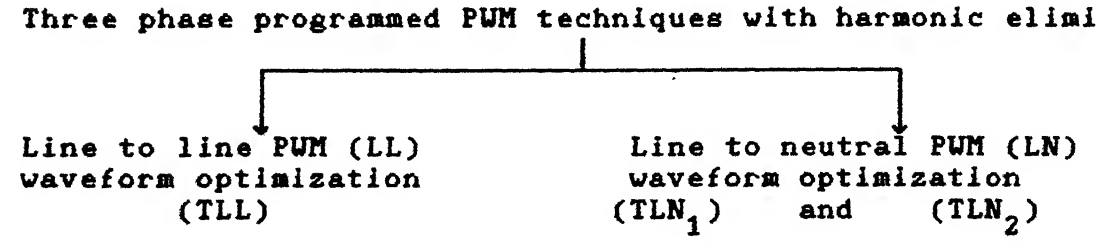

Fig. 3.4 Three phase programmed PWM techniques

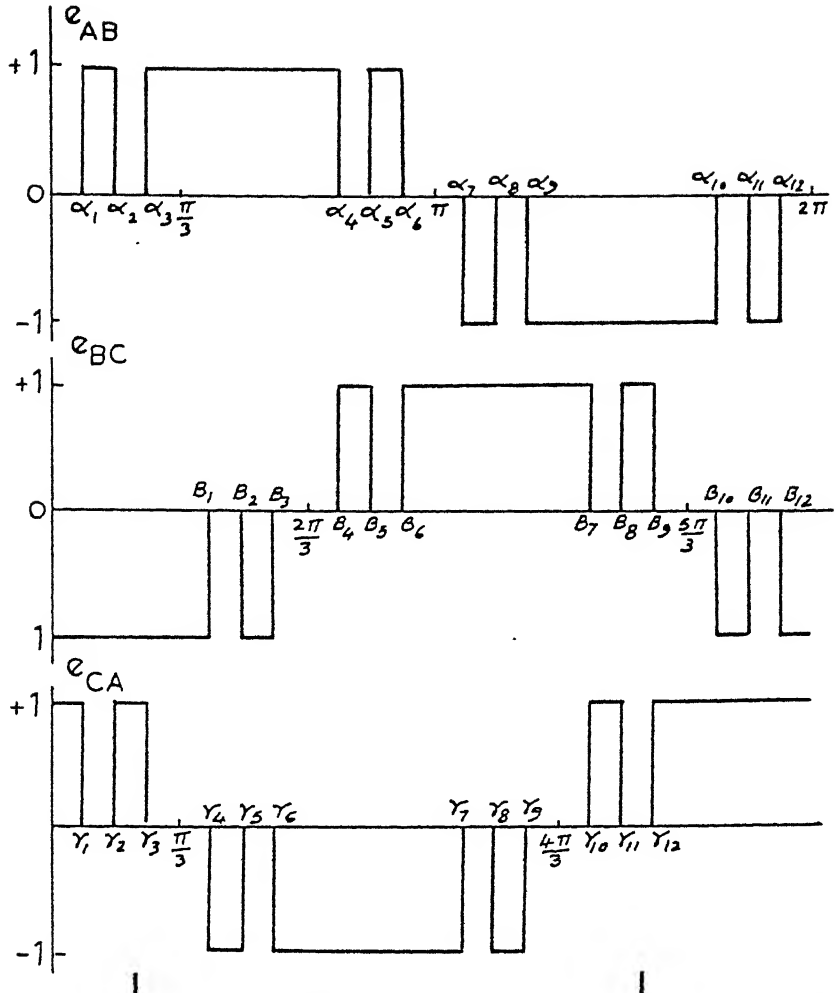

	$\beta_1 = 120 - \alpha_3$	$\gamma_1 = 60 - \alpha_3$
	$\beta_2 = 120 - \alpha_2$	$\gamma_2 = 60 - \alpha_2$
	$\beta_3 = 120 - \alpha_1$	$\gamma_3 = 60 - \alpha_1$
$= 180 - \alpha_3$	$\beta_4 = 120 + \alpha_1$	$\gamma_4 = 60 + \alpha_1$
$= 180 - \alpha_2$	$\beta_5 = 120 + \alpha_2$	$\gamma_5 = 60 + \alpha_2$
$= 180 - \alpha_1$	$\beta_6 = 120 + \alpha_3$	$\gamma_6 = 60 + \alpha_3$
$= 180 + \alpha_1$	$\beta_7 = 300 - \alpha_3$	$\gamma_7 = 240 - \alpha_3$
$= 180 + \alpha_2$	$\beta_8 = 300 - \alpha_2$	$\gamma_8 = 240 - \alpha_2$
$= 180 + \alpha_3$	$\beta_9 = 300 - \alpha_1$	$\gamma_9 = 240 - \alpha_1$
$= 360 - \alpha_3$	$\beta_{10} = 300 + \alpha_1$	$\gamma_{10} = 240 + \alpha_1$
$= 360 - \alpha_2$	$\beta_{11} = 300 + \alpha_2$	$\gamma_{11} = 240 + \alpha_2$
$= 360 - \alpha_1$	$\beta_{12} = 300 + \alpha_3$	$\gamma_{12} = 240 - \alpha_3$

Fig. 3.5. Quarter Wave Symmetric Three-phase Line to Line switching function

CHAPTER IV

DESIGN AND DEVELOPMENT OF A PWM AC-DC CONVERTER

In this chapter the detailed design and fabrication of three phase PWM ac-dc converter is described :

Proposed converter :

The proposed converter which consists of six GTO's is shwon in Fig. (4.1). GTO's used in the converter are GFT20B12(HITACHI), (The specifications of GFT20B12 are given in appendix I). GTO's have anode shorted emmitter structure. This structure allows low on-state voltage and high speed operation but does not have the reverse voltage blocking capability. Hence, a series diodes D_1 to D_6 are used in series with the respective GTO's to add this feature. Programmed-PWM scheme to control the output voltage and to eliminate 5^{th} and 7^{th} harmonics present in input current, is adopted.

Snubber circuit :

The GTO's are subjected to switching stresses during turn-on and turn-off. In order to protect the GTO from the switching stresses, a snubber circuit is usually connected with the GTO. The use of snubbers circuit ensures safe and reliable operation of GTO's with in the forward bias safe operating area, FBSOA. These snubbers are used for the following reasons [15]:

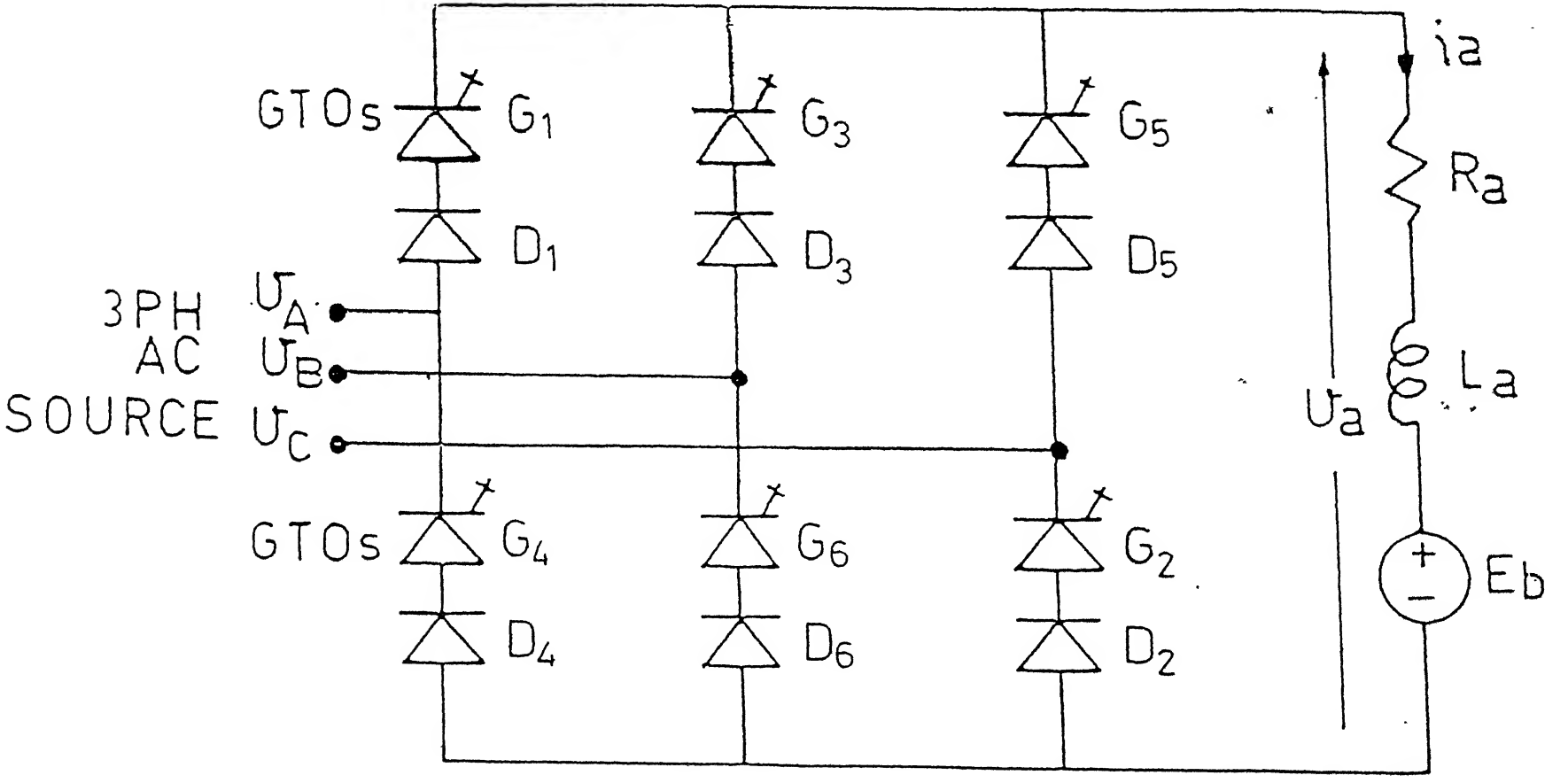

FIG.4.1 PROPOSED GTO-BASED AC-DC PWM CONVERTER

- Reduce the switching stresses on the device.
- Improve switching loci to be within the FBSOA.
- Reduce the power loss (heatsink temperature) in the swithces.
- Improve the overload and short-circuit capabilities.
- Reduce Radio frequency interference generated in the converter.
- Reduce the reverse recovery currents in the freewheeling diodes.
- Reduce over-voltage across the freewheeling diodes.
- Reduce the overall losses and improve effeciency.

Fig. (4.2) shows the snubber circuit connected with the GTO. Where L_1 represents the stray and effective external circuit inductance. This inductance serves to limit the rate of rise current during turn-on time. Hence it is called as the turn-on snubber. Diode-Resistor-Capacitor in parallel with the GTO is known as the turn-off snubber. The values of snubber circuit elements are given in Appendix II.

Effect of Source Inductance :

Due to the presence of source inductance on the ac side of the converter, an over-voltage appears across the device when the source current is interrupted by the GTO.

The magnitude of over-voltage depends on the value of source inductance and the magnitude of interrupted current.

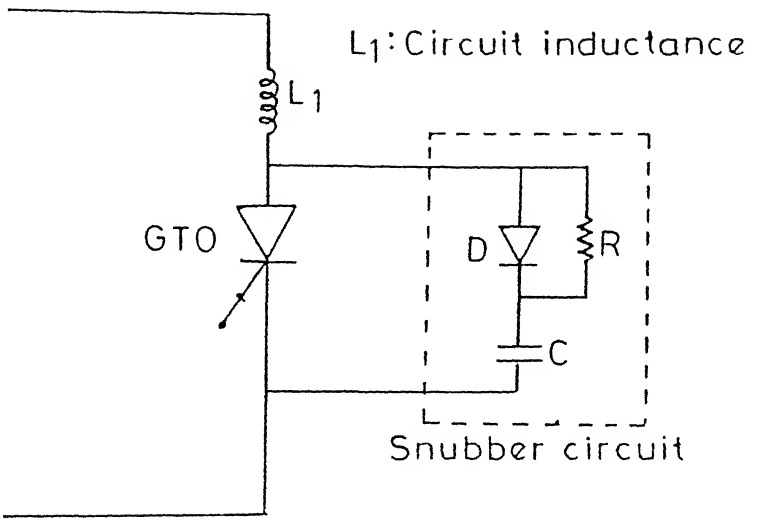

FIG. 4·2 GTO SNUBBER CIRCUIT

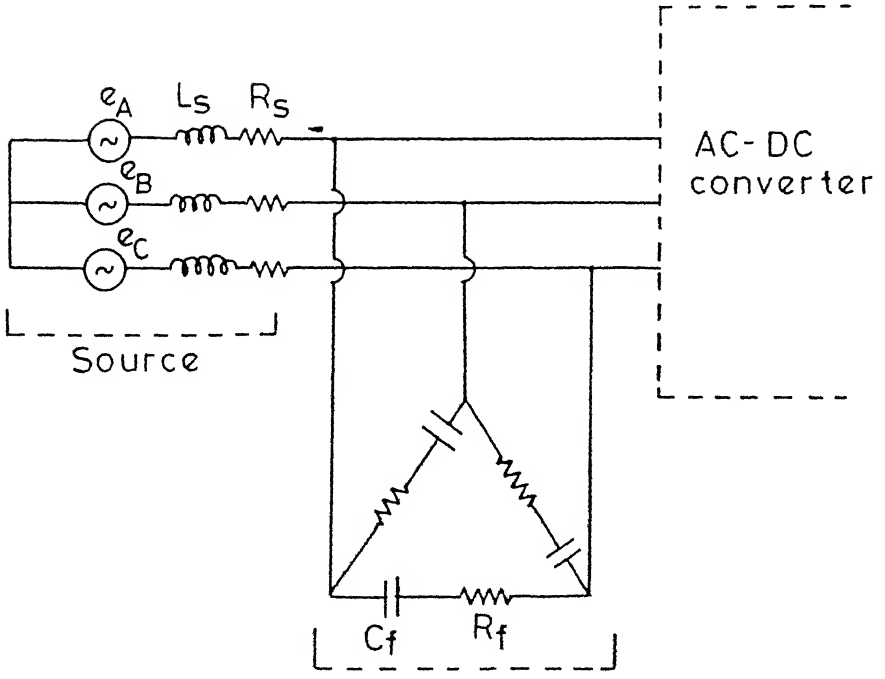

FIG.4·3 SUPPRESSION OF OVER-VOLTAGE BY RC FILTER

Increasing the size of sunbber capacitor in order to suppress the over-voltage may not be appropriate as it would also increase the losses in the device. A capacitor, C_f is used across the source terminals to take care of the source inductance separately as shown in Fig. (4.3). The value of the capacitor, C_f must be not very large as it would unduely load the source by drawing large reactive power permanently from it. Also, its value is such that its resonance frequency should not coincide with either output pulse frequency of the converter or any of the harmonics of line current. Resistor, R_f is used in series with C_f to provide damping. The values of R_f and C_f are given in Appendix II. The complete circuit of the proposed converter is shown in Fig. (4.4).

Drive Circuit :

The low power and low volttage control circuit is electically isolated from the high power circuit (or power converter circuit) for the safety of control circuit.

In this thesis, opto-coupler (MTC2E) is used to provide isolation between the control circuit and the power circuit of the converter. The block diagram representation of the driver circuit is shown in Fig. (4.5) and the details of the GTO drive circuit is shown in Fig.(4.6). The values of the circuit elements used in the drive circuit are given in appendix III. The turn-on and turn-off signals in Fig. (4.6) are complementry to each other. The drive circuit is provided with separate

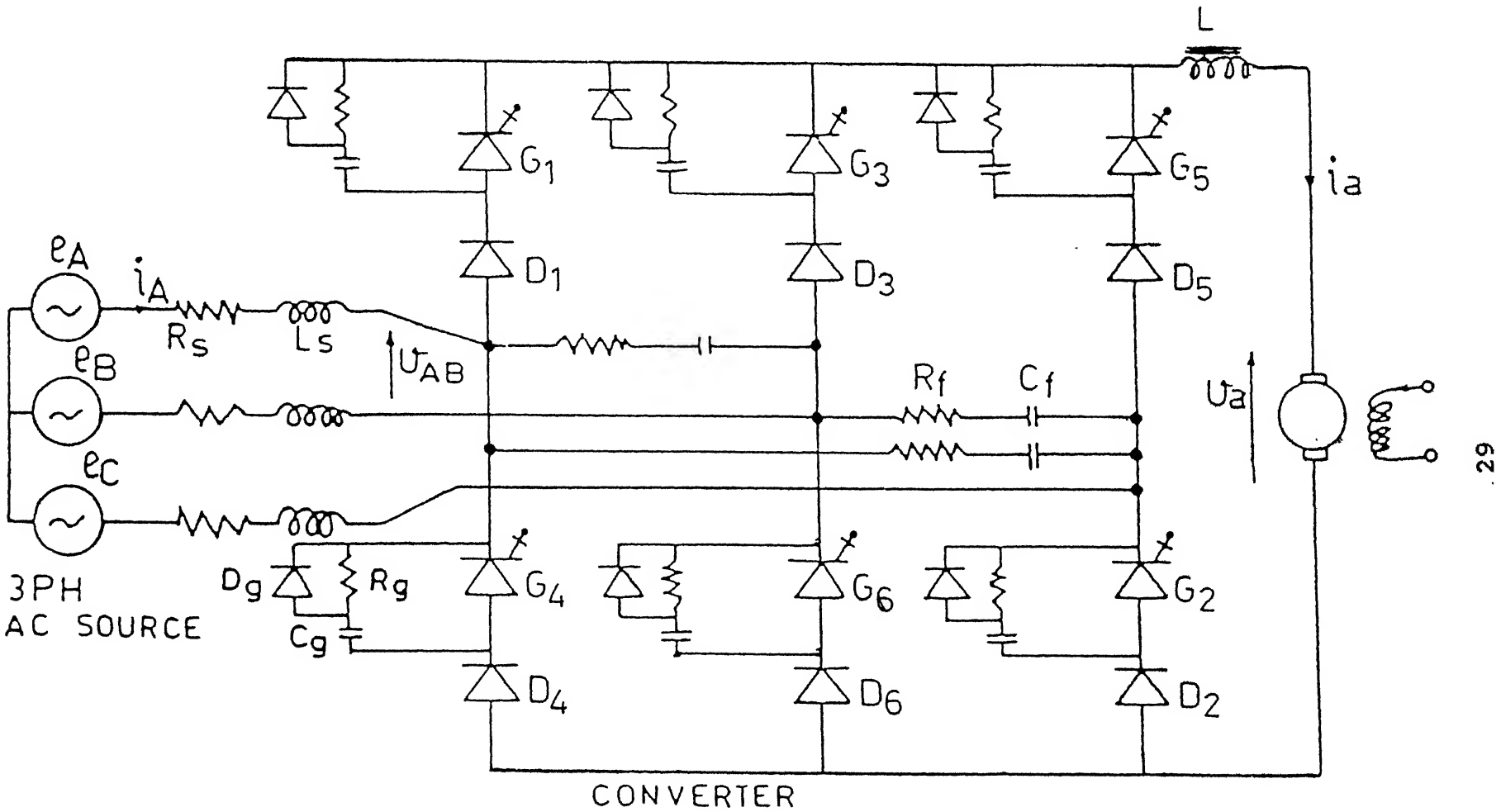
L
G1
G3
G5
ia
eA
iA
D1
D3
D5
Rs
Ls
eB
UAB
Rf
Cf
Ua
eC
3PH
AC SOURCE
Dg
Rg
Cg
G4
G6
G2
D4
D6
D2
CONVERTER

29

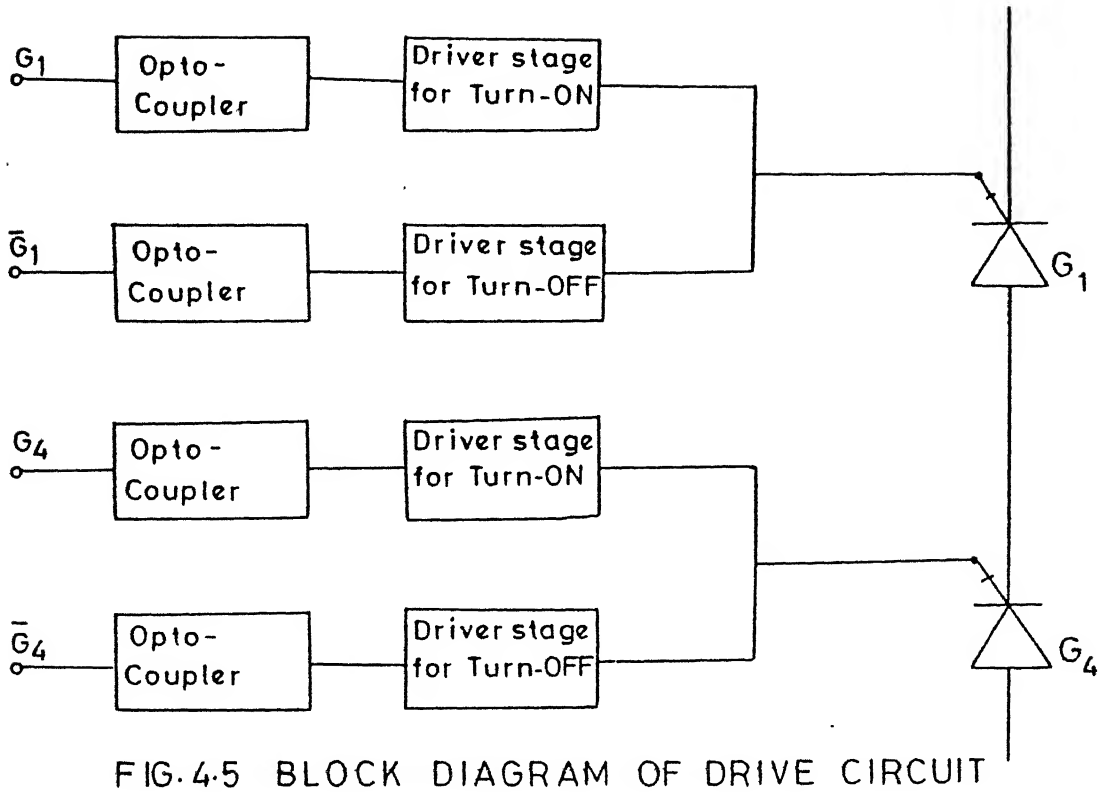

FIG.4.5 BLOCK DIAGRAM OF DRIVE CIRCUIT

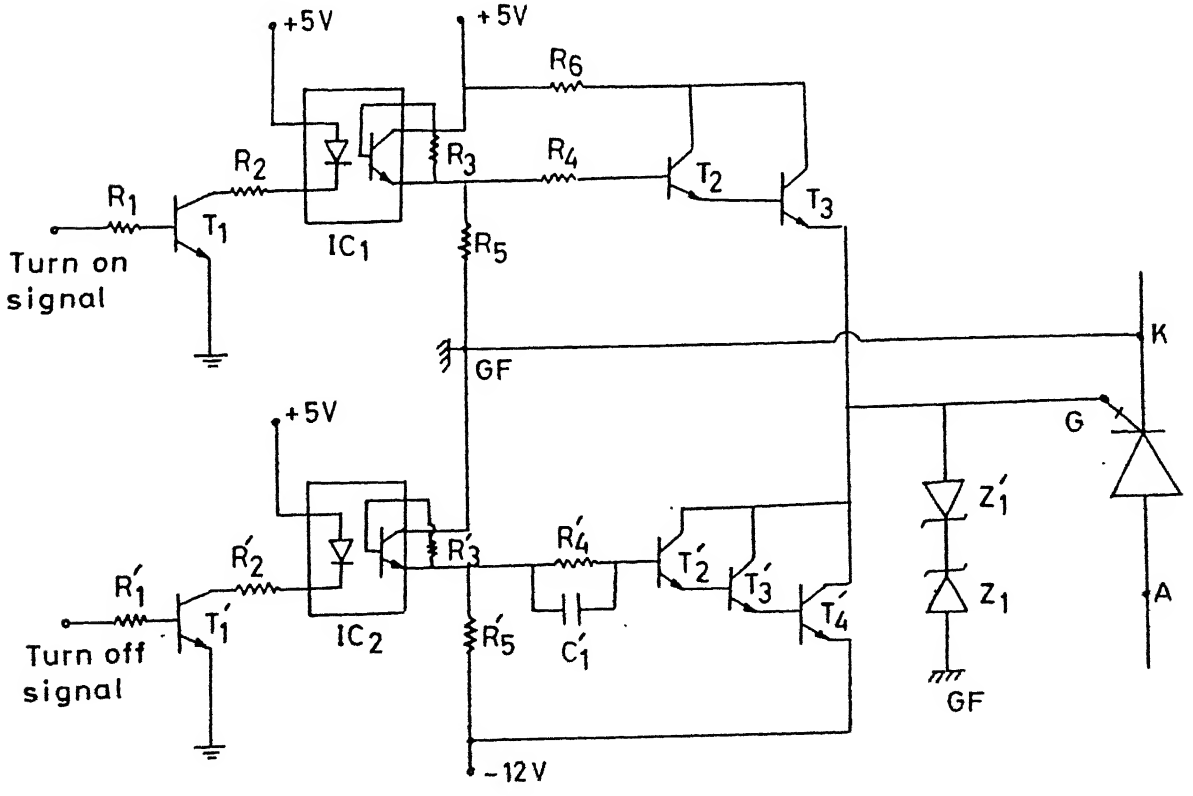

FIG.4.6 GTO DRIVE CIRCUIT

ower supplies (+5 V, -12V). These are obtained from the oltage regulators (7805) and (LM337) respectively.

ontrol Circuit :

Digital technique is used to implement the programmed PPWM technique. The block diagram of proposed digital control scheme is shown in Fig. (4.7). It consists of :

(1) Erasable programmable read only memory, EPROM.
(2) Phase-Locked Loop, PLL and frequency divider.
(3) Pulse number generation counter.
(4) Logic circuit, which consists of analog to digital converter, zero-crossing detector and comparators.

The waveforms shown in Fig. (4.8) illustrate the operation of control circuit. The logic expressions are used to obtain the gating signals are given in appendix IV.

The triggering/extinction angles are computed theoretically over the entire output range and stored in the EPROM (27256). Nine of the sixteen address lines of the EPROM are addressed by the counter (CD4040) and the remaining are by analog to digital conerter, ADC (AD7574).

The control voltage, V_c varies between zero to +2.5 V. The entire control voltage range is discretized into 64 digital levels using 8-bit analog to digital converter, ADC (AD7574).

A synchronizing signal is obtained from phase A is transformed into square wave signal by using a zero-crossing detector, ZCD (μA741). This 50 Hz signal is used as a reference signal for PLL. Since one cycle of voltage waverform is divided into 512 parts, a divide by 512 counter using three 4-bit programmable binary counters (74191) is used as a multiplier in the PLL circuit. The output of PLL is used as a clock signal to the counter (CD4040). This technique synchronizes the triggering signals with the supply. A pulse of duration 20 μSec is obtained at every zero crossing of the line voltage using mono-stable (4047). The output of monostable is used as clock signal to the ADC. The outputs of the counter (CD4040) and of the ADC, control the address lines of the EPROM. Using the output pulses from the EPROM and comparators (comparing e_A, e_B and e_C), the gating pulses for the GTO's are obtained.

Gating pattern :

GTO's are triggered using unsymmtrical type of gating pattern which is shwon in Fig.(4.9).

In this case GTO's of the upper limb (G_1, G_3, and G_5) of the converter are turned-on and off five times in one cycle of the respective phase voltage, while those in the lower limb (G_4, G_6, and G_2) are turned-on and off once in every cycle of the respective phase voltage. These GTO's conduct for 120° per cycle.

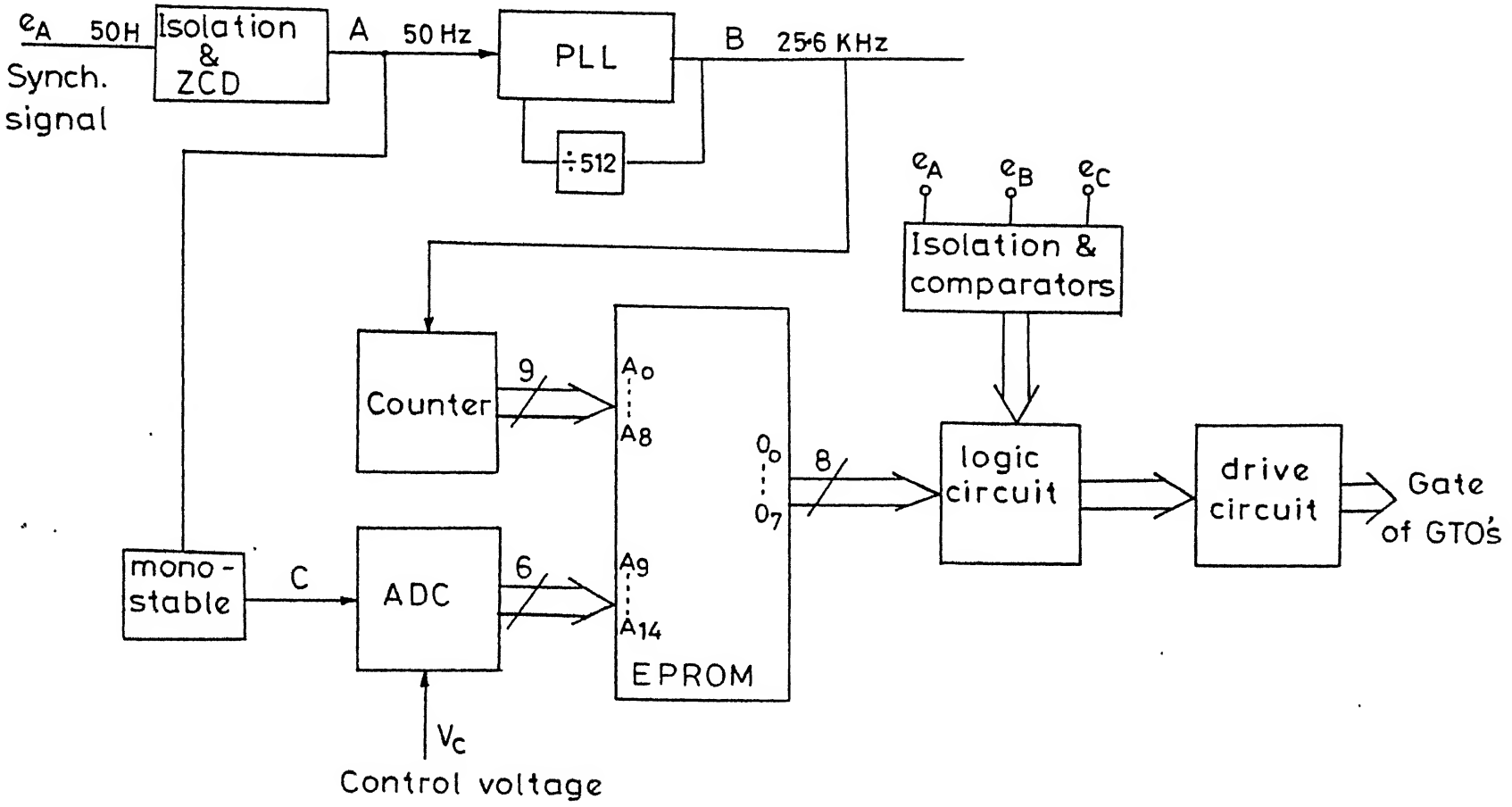

FIG. 4·7 BLOCK DIAGRAM OF CONTROL CIRCUIT

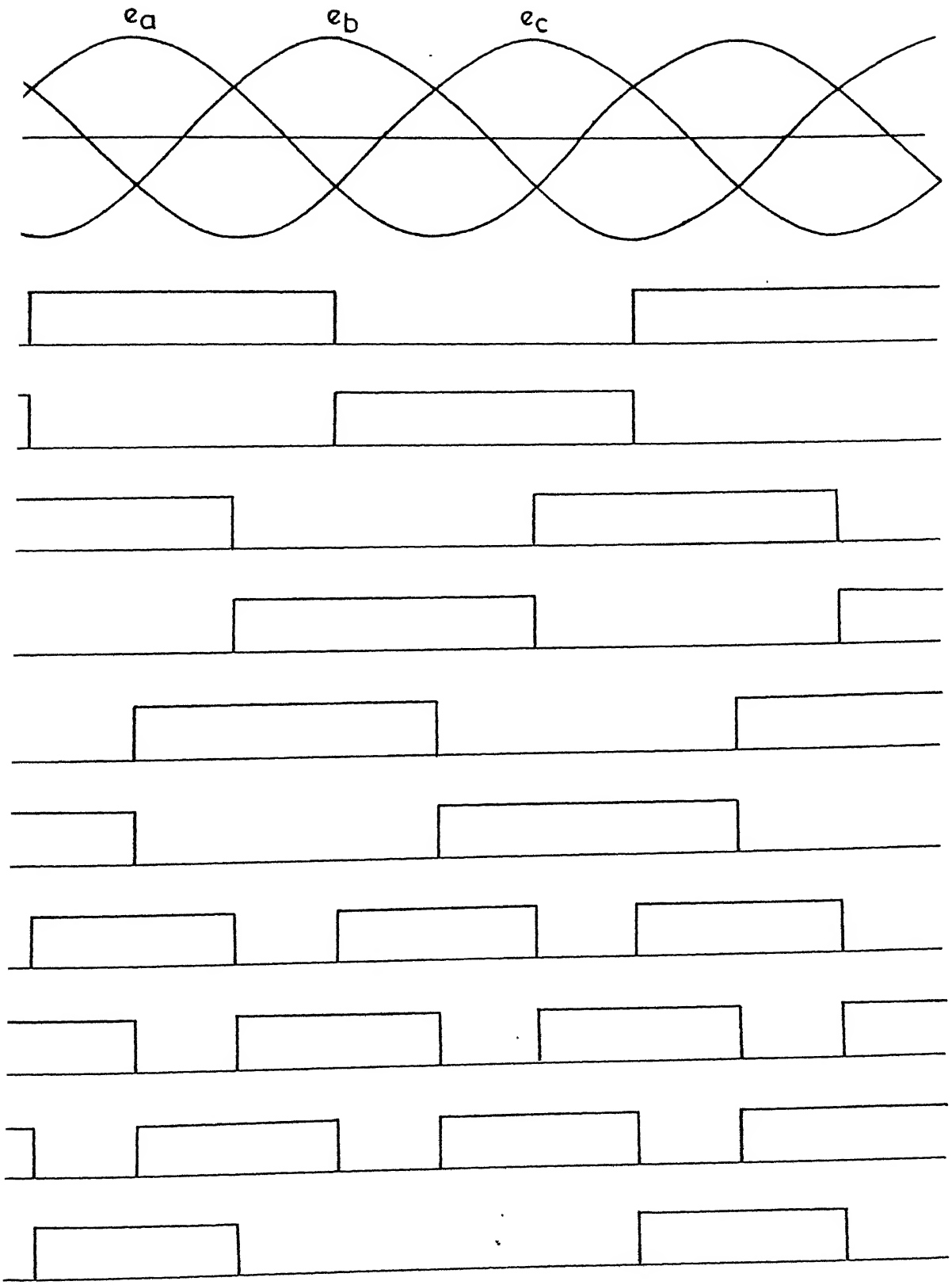

FIG·4·8 WAVEFORMS OF SIGNALS AT VARIOUS STAGES OF CONTROL CIRCUIT

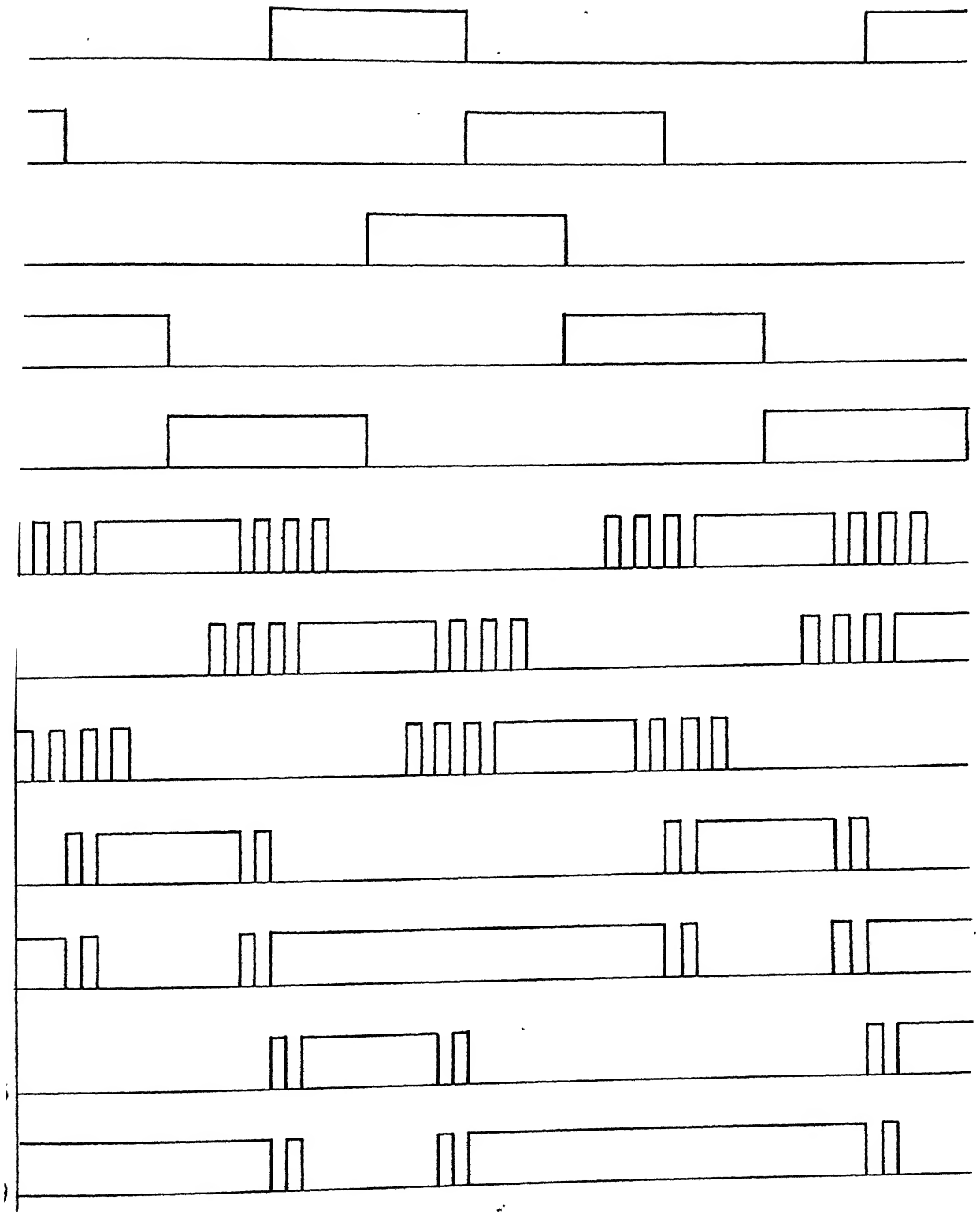

FIG.4.8 (CONTD.)

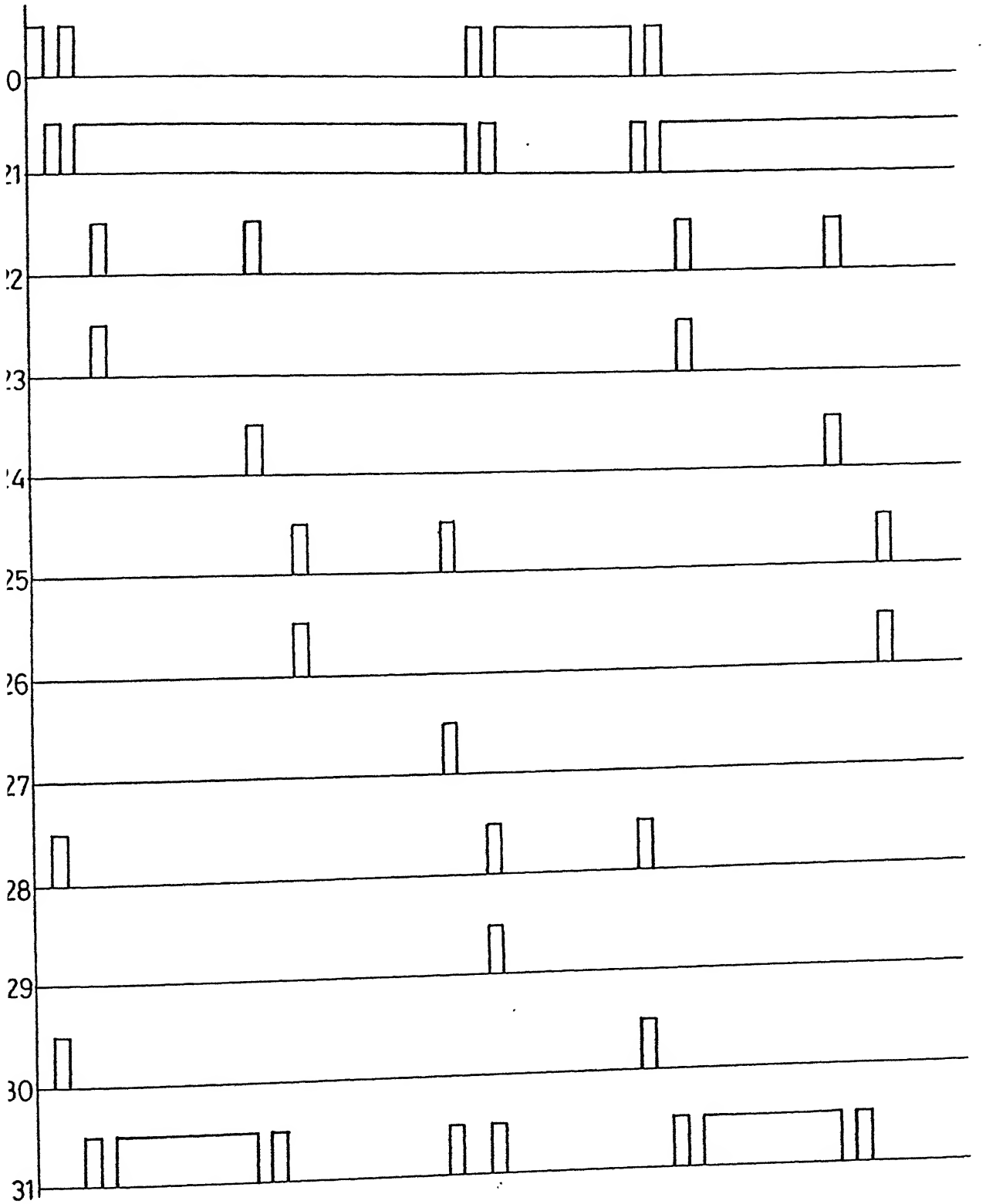

FIG. 4·8 (CONTD.)

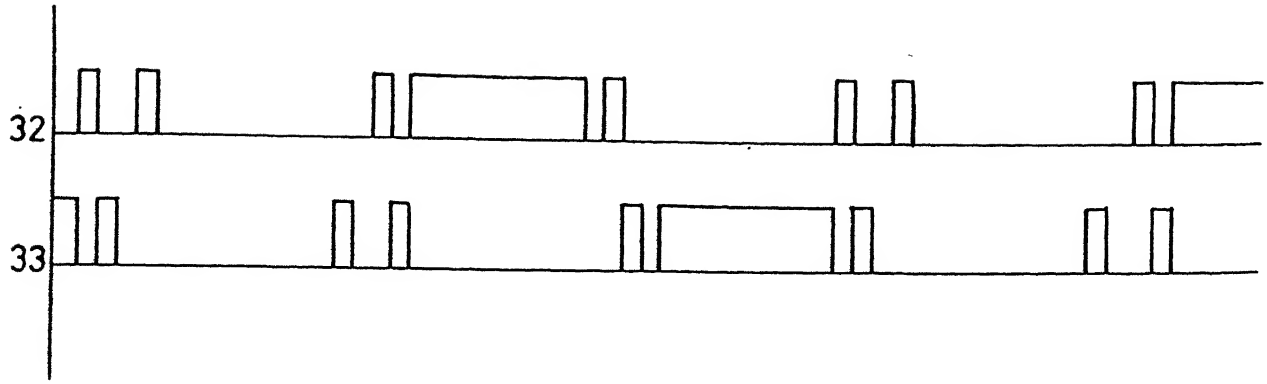

FIG. 4·8 (CONTD.)

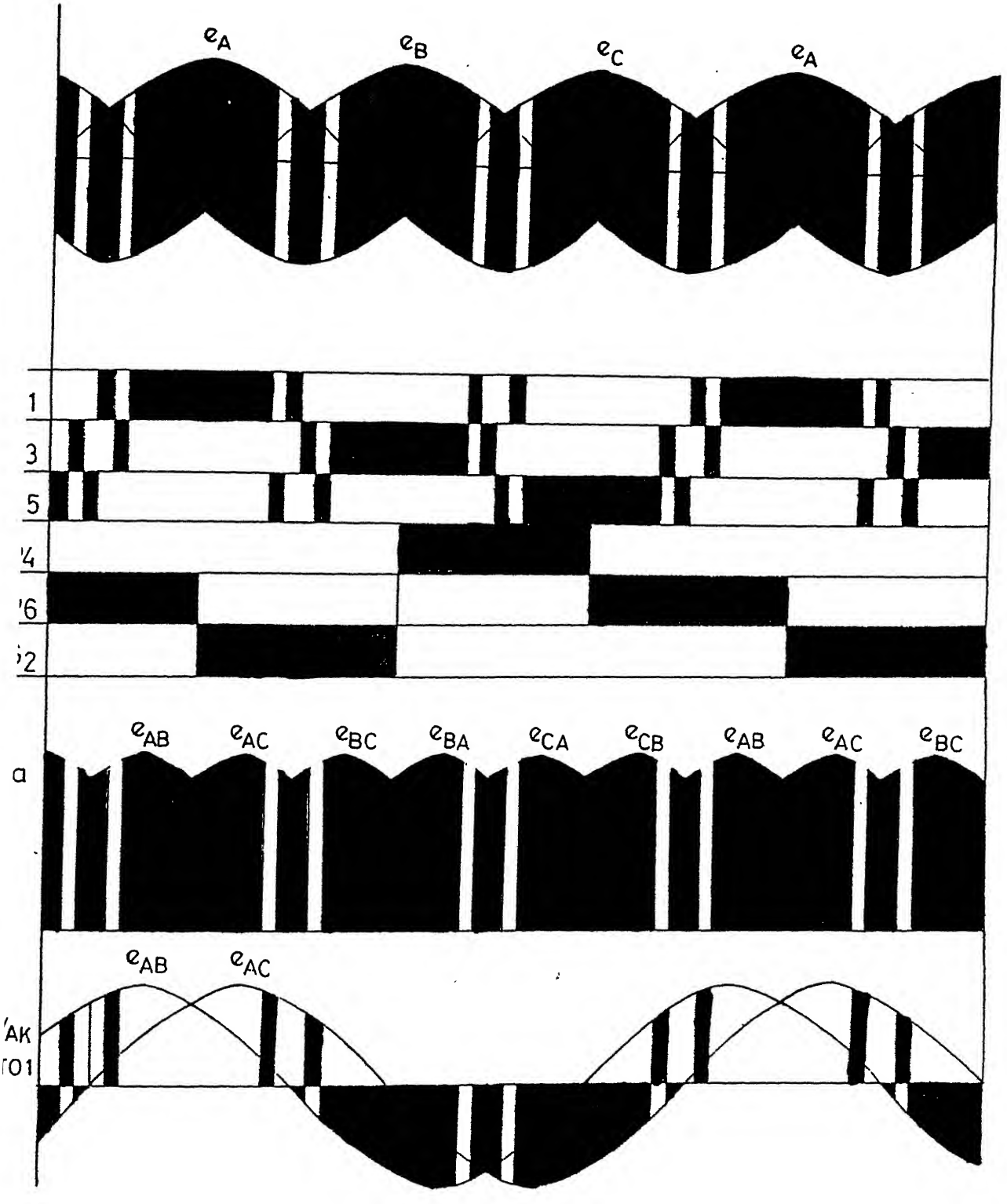

FIG·4·9 GATING PATTERN, OUTPUT VOLTAGE AND VOLTAGE ACROSS G_1

CHAPTER V

PERFORMANCE EVALUATION OF THE CONVERTER FED DC MOTOR

.1 The experimental setup :

The converter discussed in chapter IV is fabricated and tested with a separately excited dc motor. The complete drive system is shown in Fig. (5.1). Where,

R_1 : used for measuring the input AC current

R_2 : used for measuring the output DC current

R_3 : Resistive load for dc generator

And the photograph of the setup is shown in Fig. (5.2). The specifications of the drive system are given in appendix V.

5.2 Load test and experimental results :

5.2.1 Speed-Torque characteristics :

The speed-torque characteristics are shown in Fig. (5.3). The curves indicate motoring operation. The armature current is almost continuous because of multipulse width modulation. It can be seen from the Fig. (5.3) that the speed increases with an increase in the output voltage of the converter (armature voltage), and for a given armature voltage, the speed decreases with an increase in torque.

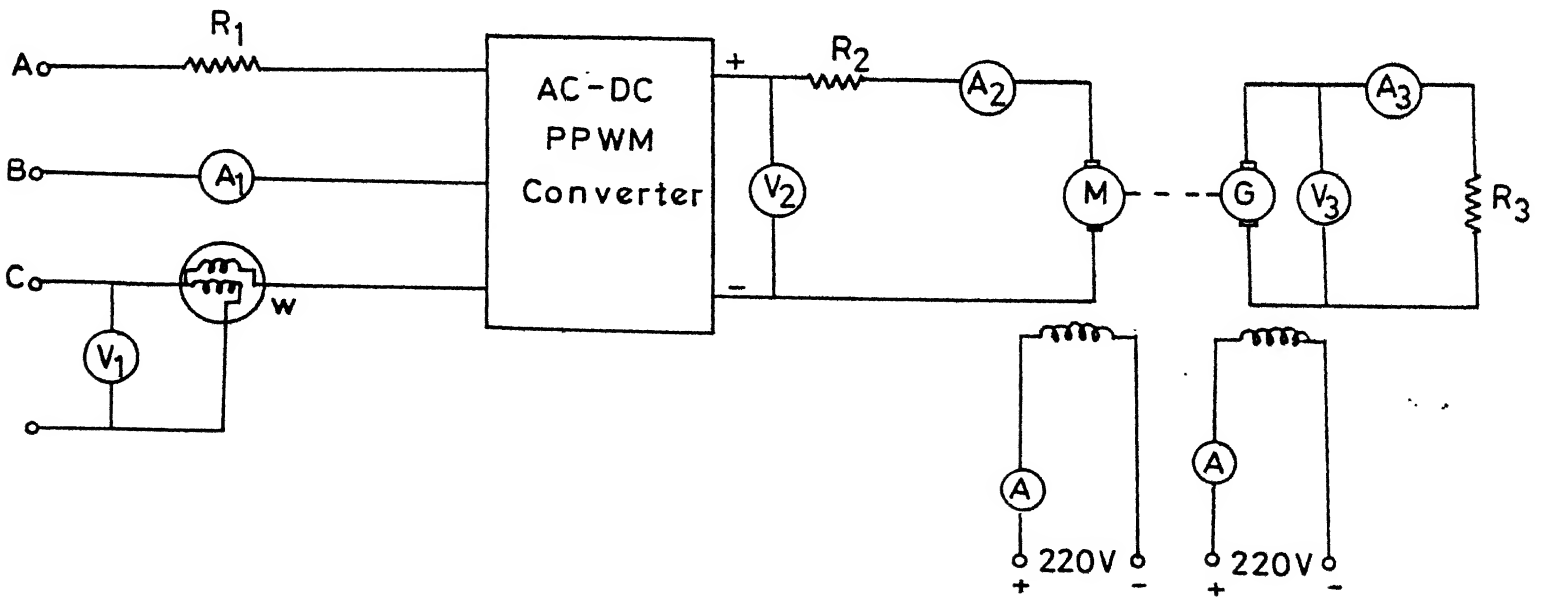

FIG. 5.1 THE COMPLETE DRIVE SYSTEM

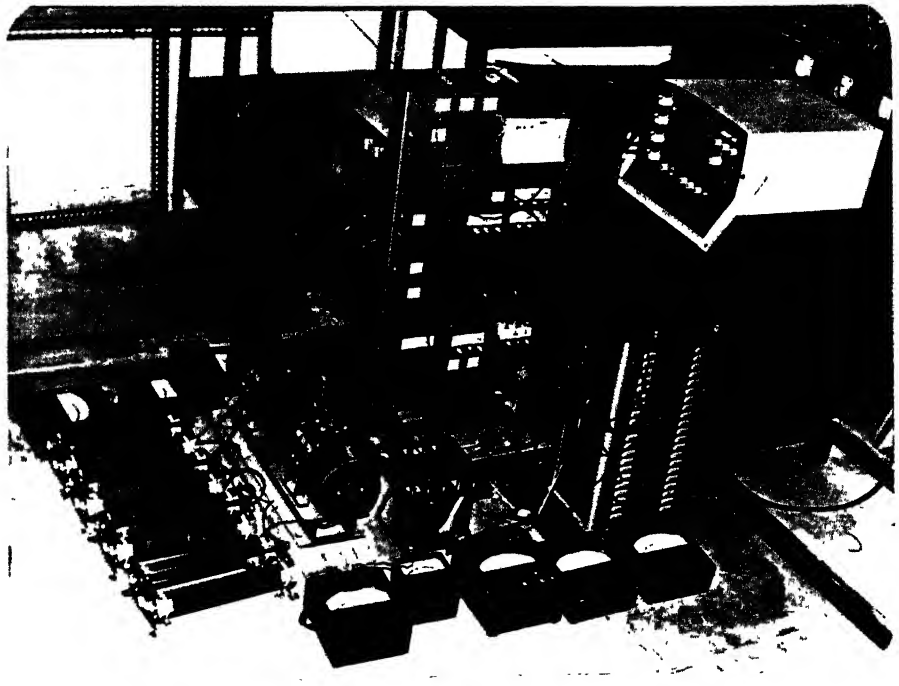

Fig. (5.2)

The setup of the system

Input power factor versus output voltage :

Fig. (5.4) shows the input power factor versus the output voltage of the converter. The displacement factor is unity for all values of output voltage. It can be seen that the power factor increases with an increase in torque. For a given torque, the power factor slightly increases with an increase in the output voltage.

Experimental oscillograms :

Experimental oscillograms are obtained from the setup to verify the basic principles of the PPWM technique, input and output performances.

Unsymmetrical gating pattern was realized and corresponding oscillograms are shown in Figs. (5.5A), (5.5B), and (5.5C) for the modulation index equal to 0.2. These figures show the input voltage and gating pulses for six GTO's, G_1-G_6.

Oscillogram of the voltage across GTO, G_1 is shown in Figs. (5.6), (5.7) and (5.8). It can be seen that the voltage across GTO, G_1 during ON period of G_1 is zero and during ON period of G_3 and G_5, it is e_{AB} and e_{AC} respectively.

Oscillogram of the output voltage of the converter is shown in Fig. (5.6). It can be seen the output voltage is zero when the two switches (GTO's) in the same leg conduct (ON period). While it is equal to the line voltage, when two switches in the different legs conduct.

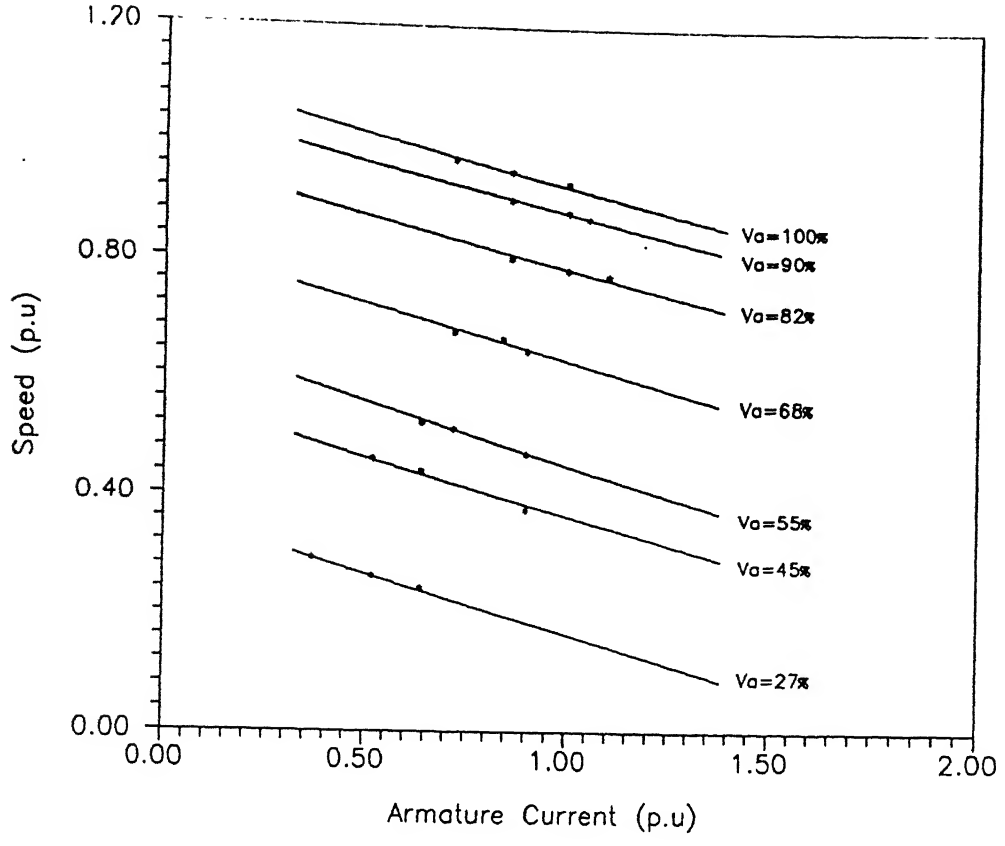

Fig. 5·3 Speed–Torque Characteristics

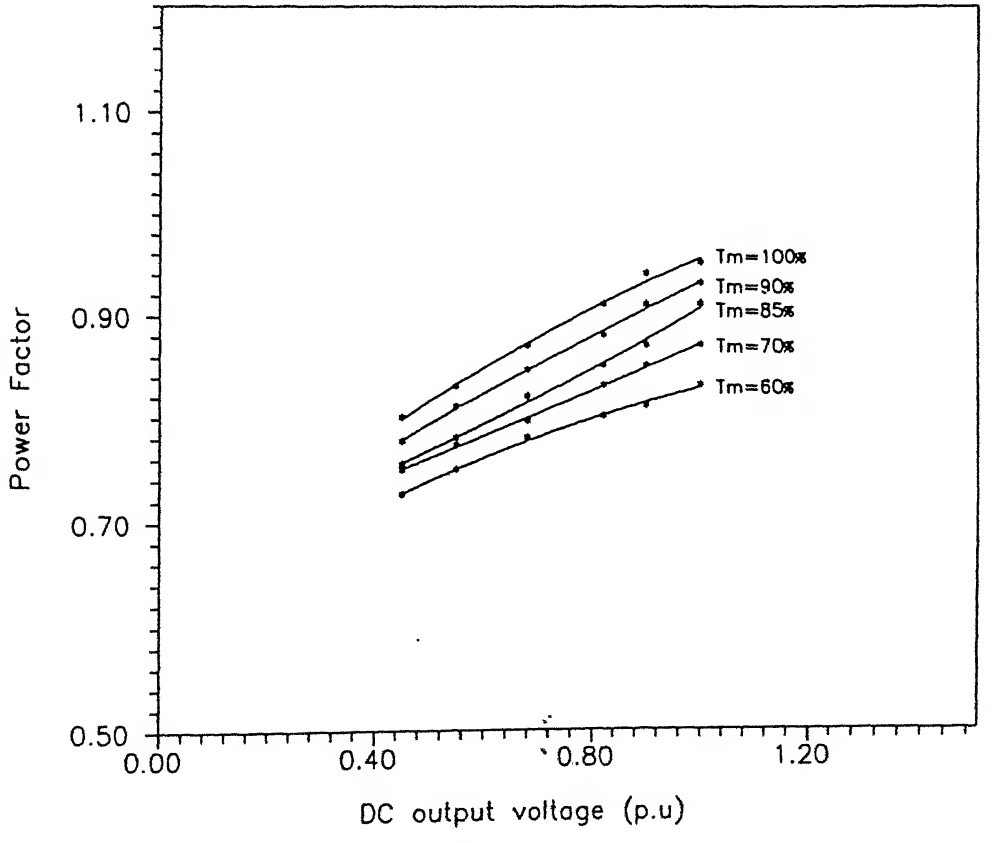

Fig. 5·4 Power Factor versus DC Output Voltage

Oscillogram of the output current is shown in Figs. (5.6) and (5.7). It can be seen that the output current is continuous.

Oscillogram of the input current is shown in Fig. (5.7). It can be seen that the input current is equal to load current during power interval and it is equal to zero during the freewheeling interval.

Oscillogram of the voltage across GTO, G_4 is shown in Fig. (5.8). It can be seen that the voltage across G_4 during ON period of G_4 is zero and during ON period of G_6 and G_2, it is e_{BA} and e_{BC} respectively.

The oscillograms in Figs. (5.9), (5.10), (5.11) and (5.12) show the gating pulses for G_1-G_6, input voltage, input current, output voltage, output current and the voltage across G_1 & G_4 for another value of modulation index 0.6.

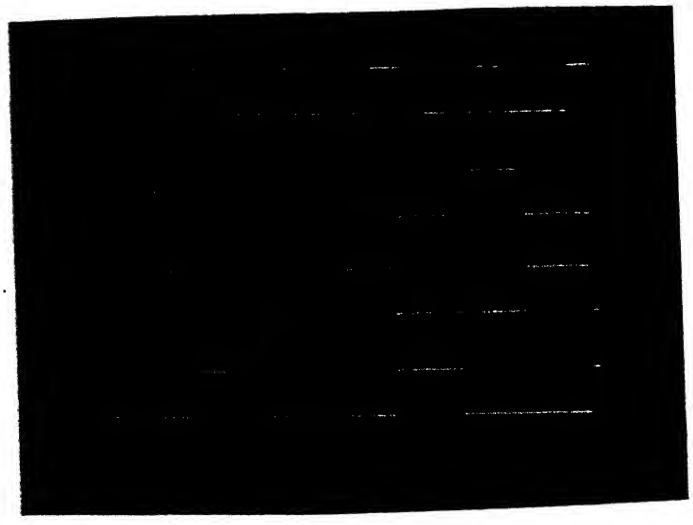

Fig. (5.5A)

(1) gating pulses for G_1 (5V/div)
(2) gating pulses for G_4 (5V/div)
(3) gating pulses for G_6 (5V/div)
(4) gating pulses for G_2 (5V/div)
Time Scale (5ms/div)

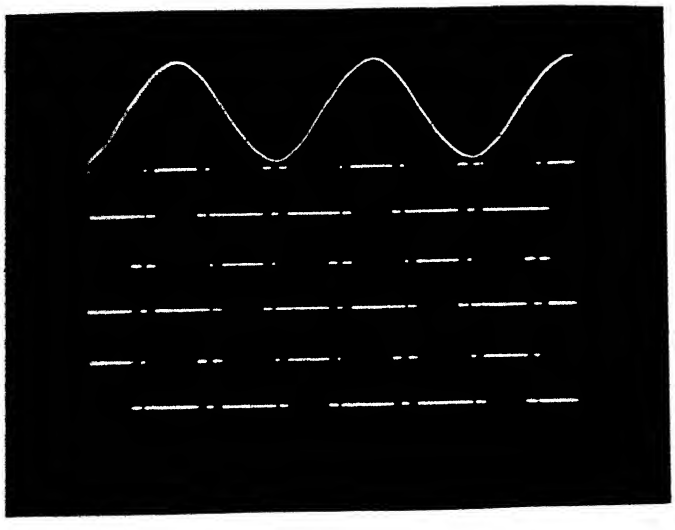

Fig. (5.5B)

(1) input voltage e_A (5v/div)
(2) gatting pulses for G_1 (5V/div)
(3) gatting pulses for G_3 (5V/div)
(4) gatting pulses for G_5 (5V/div)
Time Scale (5ms/div)

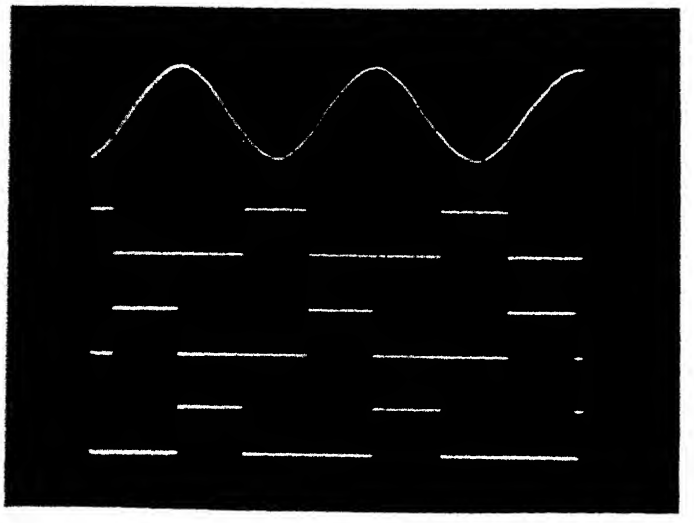

Fig. (5.5C)

(1) input voltage e_a (5v/div)
(2) gating pulses for G_4 (5V/div)
(3) gating pulses for G_6 (5V/div)
(4) gating pulses for G_2 (5V/div)
Time Scale (5ms/div)

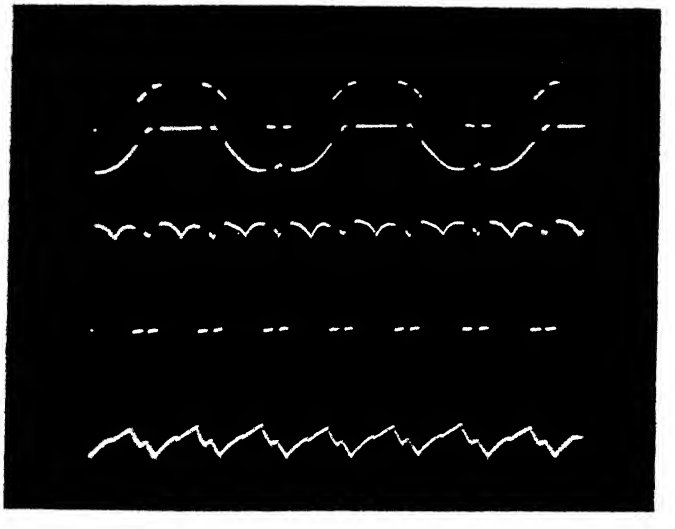

Fig. (5.6)

(1) Voltage across G_1 (50 v/div)
(2) output voltage v_a (50 v/div)
(3) output current i_a (6.17A/div)
Time Scale (5ms/div)

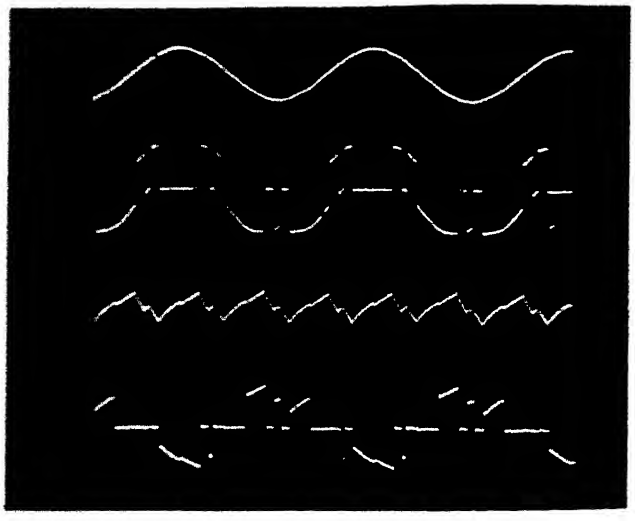

Fig. (5.7)

(1) input voltage e_A (50 v/div)
(2) voltage across G_1 (50 v/div)
(3) output current i_a (6.17A/div)
(4) input current i_A (7.4A/div)
Time Scale (5ms/div)

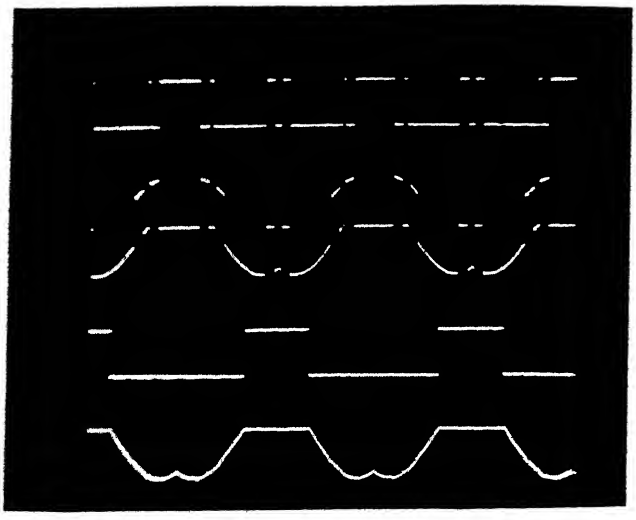

Fig. (5.8)

(1) gating pulses for G_1 (5V/div)
(2) Voltage across G_1 (50V/div)
(3) gating pulses for G_4 (5V/div)
(4) voltage across G_4 (50V/div)
Time Scale (5ms/div)

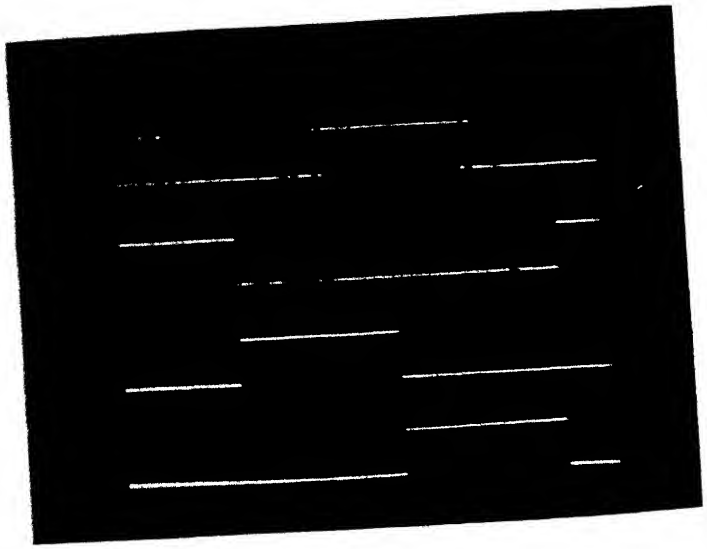

Fig. (5.9A)

(1) gating pulses for G_1 (5V/div)
(2) gating pulses for G_4 (5V/div)
(3) gating pulses for G_6 (5V/div)
(4) gating pulses for G_2 (5V/div)
Time Scale (2ms/div)

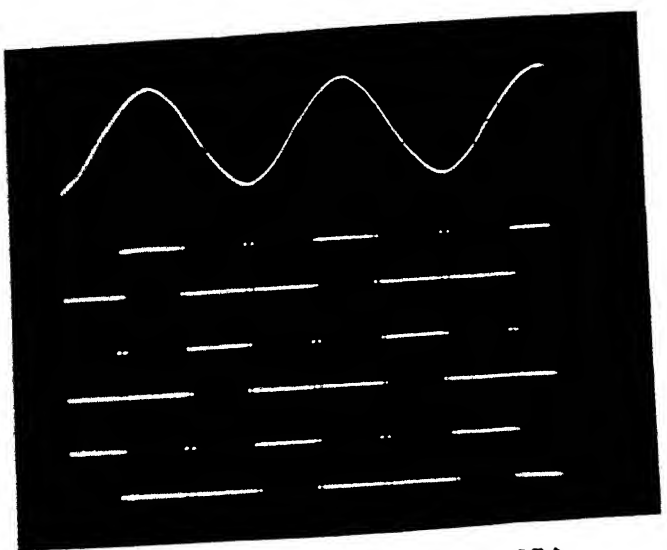

Fig. (5.9B)

(1) input voltage e_A (5v/div)
(2) gating pulses for G_1 (5V/div)
(3) gating pulses for G_3 (5V/div)
(4) gating pulses for G_5 (5V/div)
Time Scale (5ms/div)

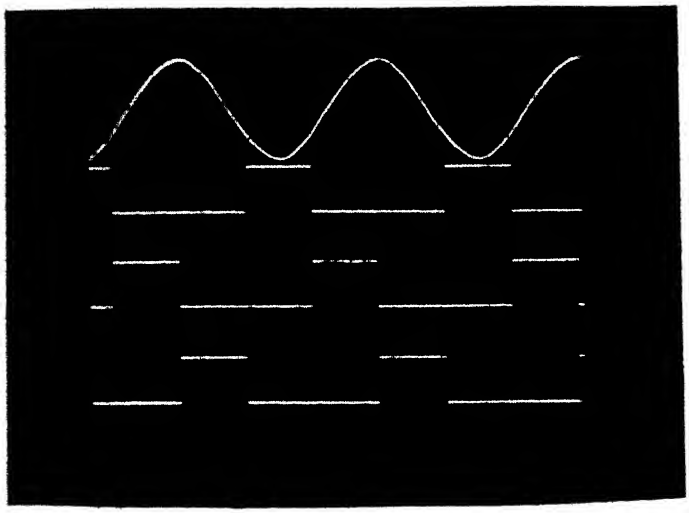

Fig. (5.9C)

(1) input voltage e_A (5v/div)
(2) gating pulses for G_4 (5V/div)
(3) gating pulses for G_6 (5V/div)
(4) gating pulses for G_2 (5V/div)
Time Scale (5ms/div)

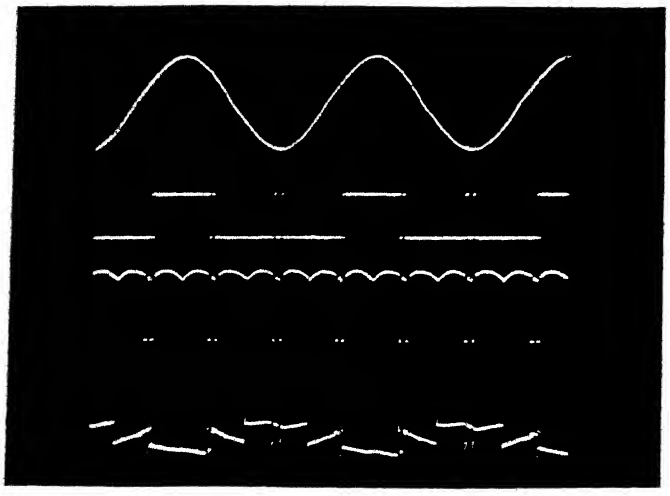

Fig. (5.10)

(1) input voltage e_A (5v/div)
(2) gating pulses for G_1 (5V/div)
(3) output voltage v (50V/div)
(4) input current i_a (7.4 A/div)
Time Scale (5ms/div)

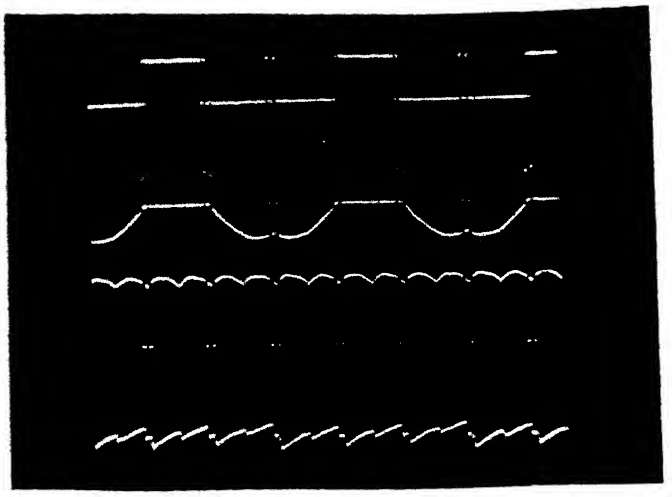

Fig. (5.11)

(1)	gating pulses for	G_1	(5v/div)
(2)	voltage across	G_1	(100v/div)
(3)	output voltage	v_a	(50v/div)
(4)	output current	i_a	(6.17 A/div)
	Time Scale	(5ms/div)	

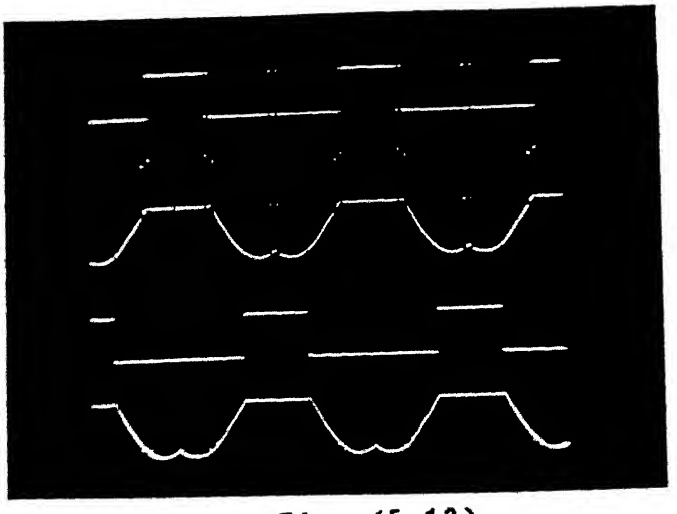

Fig. (5.12)

(1)	gating pulses for	G_1	(5v/div)
(2)	voltage across	G_1	(50v/div)
(3)	gating pulses for	G_4	(5v/div)
(4)	voltage across	G_4	(50 v/div)
	Time Scale	(5ms/div)	

CHAPTER VI

CONCLUSIONS

In this thesis a GTO-based three phase ac-dc PWM converter is analyzed, constructed and experimentally tested with a dc motor.

The experimental results are in close agreement with theoretically predicted results. The study reveals that the three phase PPWM ac-dc converter-controlled separately excited dc motor is desirable for industrial applications involving large horsepower drives owing to improved performance. The displacement factor is unity and there is a significant improvement in the power factor.

The use of gate turn-off thyristor, GTO substantially reduces volume and weight of the converter. However, it needs a greater care to be taken while desigining the drive and the snubber circuits. The effect of source inductance becomes more prominent with the increase in load current. The drive circuit must be very near to the converter assembly and use of long wires must be avoided. The snubber circuit and drive circuit are required for reliable operation of the converter.

REFERENCES

1] G.K. Dubey , S.R. Doradla, A. Joshi, R.M.K. Sinha, "Thyristorised Power Controllers", WILEY EASTERN LIMITED, 1986.

2] G.K. Dubey, "PWM self commutated Ac-Dc converter", IE(I) Journal-EL, Volume 70, June 1989, pp. 46-54.

3] W. McMurrey, "A Study of asymmetrical gating for phase-controlled converter", IEEE Trans. Ind. Appl., Vol. IA-8, No. 3, May/June 1972, pp. 289-295.

4] S. Mukhopadhyaya, "A new concept for improving the performance of phase-controlled converter", IEEE Trans. Ind. Appl., Vol. IA-14, No. 6, Nov./Dec. 1978, pp. 584-603.

5] V.R. Stefanovic, "Power factor improvement with a modified phase-controlled converter", IEEE Trans. Ind. Appl., Vol. IA-15, No. 2, March/April 1979, pp. 193-200.

[6] T. Ohnishi and H. Okitsu, "Bais voltage controlled three-phase converter with high power factor", IEEE Trans. Ind. Appl., Vol. IA-16, No. 5, Sep./Oct. 1980, pp. 700-706.

[7] P. Enjeti, Ph.D. Ziogas and J. Lindsay, "Programmed PWM Techniques to Eliminate Harmonics : A Critical Evaluation", IEEE Trans. Ind. Appl., Vol. IA-26, No. 2, March/April 1990,

[8] S.R. Doradla, C. Nagamani, and S. Sanyal, "A sinusoidal pulse-width modulated Three-phase AC-DC Converter. fed dc motor drive", IEEE Trans. Ind. Appl., Vol. IA-21, No. 6, Nov./Dec. 1985, pp. 1394-1408.

[9] N.D. Prasad, "Close loop control of PWM Ac-Dc converter fed separately excited Dc motor", M.Tech. Thesis, I.I.T. Kanpur, June 1984.

[10] H. Inaba, S. Shima, A Ueda, T. Ando, T. Kurosawa and Y Sakai, "A New Speed Control System for DC Motors Using GTO Converter and Its Applications to Elevators", IEEE Trans. Ind. Appl., Vol. IA-21, No. 2, March/April 1985, pp. 391-400.

[11] T. Kataoka, K. Kawakami, and J. Kitano, "A Pulse-width Modulated Ac-Dc Converter using GTO Thyristor", In Proc. Conf. Rec. IEEE/IAS, 1985, pp. 966-976.

[12] P. Viriya, H. Kulota, and K. Matsuse, "New PWM-controlled GTO Converter", IEEE Trans. Power Electronics, Vol. PE-2, No. 4, Oct. 1987, pp. 373-380.

.3] B.H. Khan, "GTO converter fed Dc motor drives", Ph.D. thesis IIT Kanpur, March 1988. pp. 302-316.

[4] H.S. Patel and R.G. Hoft, "Generalized Techniques of Harmonic Elimination and Voltage Control in Thyristor Inverters : Part-I- Harmonic Elimination", IEEE Trans. Ind. Appl., Vol. IA-9, No. 4, May/June 1973, pp. 310-317.

15] T. Undelan, F. Jenset, A. Steinbakk, "A snubber Configuration for Both Power Transistor and GTO PWM Inverters", in Proc. Conf. Rec. IEEE/PESC, 1984, pp. 42-53.

Appendix I

he specifications of GFT20B12 are :

epetitive Peak Off-state Voltage (V_{DRXM})	= 1200 V
epetitive Controllable On-state Current (I_{TCM})	= 20 A
MS On-state Current I_T (RMS)	= 7 A
Non-repetitive Controllable On-state Current (I_{TCMS})	= 40 A
Non-repetitive Surge On-state Current (I_{TSM})	= 65 A
I^2 T limit value	= 3.2 A^2.S
Critical Rate of Rise of On-state Current (di/dt)	= 150A/μS
Repetitive Peak Reverse Gate Voltage (V_{GRM})	= 13 V
Reverse Voltage between Anode and Cathode (V_{GRM})	= 13 V
Repetitive Average Forward Gate Power Dissipation $P_{GF(av)}$	= 1.5W
Repetitive Peak Forward Gate Power Dissipation (P_{GFM})	= 5 W
Repetitive Average Reverse Gate Power Dissipation $P_{GR(av)}$	= 2.5W
Repetitive Peak Reverse Gate Power Dissipation (P_{GRM})	= 200 W
Operating Junction Temperature (T)	= -40 to 125°C
Critical Rate of Rise of Off-state Voltage (dv/dt)	= 1000 V/μS
Holding Current (I_h)	= 200 mA
Latching Current (I_l)	= 700 mA

Appendix II

The details of source and converter are given below :

(a) Source :

1. A three-phase 50 Hz, ac supply.
2. Source Voltage : 230 V

(b) Converter :

(i) Over voltage suppression circuit elements :

R_f = 25 Ω/100 W

C_f = 0.74 μF/960 V

(ii) GTO Snubber circuit :

R_g = 100 Ω/5 W

C_g = 0.1 μF/800 V

diode : PRF 818 A (Fast recovery diode)

(iii) GTO : GFT20B12 (1200 V/7A)

(iv) Series Diode : SPR-16 A

Appendix III

Drive Circuit Elements

The Element		The Value
Resistor	$R_1 - R'_1$	3.3 KΩ 1/8 W
	$R_2 - R'_2$	150 Ω 1/8 W
	$R_3 - R'_3$	68 KΩ 1/8 W
	$R_4 - R'_4$	470 KΩ 1/8 W
	$R_5 - R'_5$	1.2 KΩ 1/8 W
	R_6	36 Ω - 10 W
Capacitor	C'_1	0.022 μF
Transistor	$T_1 - T'_1$	BC 148
	$T_2 - T'_2$	BC 148
	$T_3 - T'_3$	SL100
	T'_4	2N3055
Zener	Z_1	10 V–3 W
	Z'_1	5.1 V–3 W
Opto-Coupler	$IC_1 - IC_2$	MTC2E

Appendix IV

Signal	Logic expersssion
(1)	Compare e_A and e_C
(2)	Inverse of (1)
(3)	Compare e_A and e_B
(4)	Inverse of (3)
(5)	Compare e_B and e_C
(7)	(1) XOR (4)
(8)	(3) XOR (5)
(9)	(2) XOR (5)
(10)	(7) AND (3)
(11)	(8) AND (4)
(12)	(9) AND (6)
(13)	(7) AND (2) = G_4
(14)	(8) AND (3) = G_6
(15)	(9) AND (5) = G_2
(16)	(O_o) AND (10)
(17)	Inverse of (16)
(18)	(O_1) AND (11)
(19)	Inverse of (18)
(20)	(O_2) AND 12
(21)	Inverse of (20)
(22)	(10) AND (17)
(23)	(22) AND (14)
(24)	(22) AND (15)

(25)	(11) AND (19)
(26)	(25) AND (15)
(27)	(25) AND (13)
(28)	(12) AND (21)
(29)	(28) AND (13)
(30)	(28) AND (14)
(31)	(16) OR (27) OR (29) = G_1
(32)	(18) OR (23) OR (30) = G_3
(33)	(20) OR (24) OR (26) = G_5

Appendix V

THE SPECIFICATIONS OF THE DRIVE SYSTEM

) **Resistors :**

(i) R_1 = 0.27 Ω/25 W

(ii) R_2 = 8 Ω/5 A

(iii) R_3 = 0 - 100 Ω/5 A

) **The dc Motor :**

Rated voltage 220 V — field voltage 220 V

Rated current 2.2 A — field current 0.25 A

Rated power 0.5 hp

Rated speed 1500 rpm

Armature Resistor R_a = 12 Ω

) **The dc Generator :**

Rated voltage 220 V — field voltage 220 V

Rated current 2.2 A — field current 0.25 A

Rated power 0.5 hp

Rated speed 1500 rpm

Armature Resistor R_a = 12 Ω

Appendix VI : The Commutating Angles α_1, α_2, α_3

V_1 (%)	α_1 (rad)	α_2 (rad)	α_3 (rad)
0.10	0.5	0.54	1.024
0.12	0.495	0.543	1.02
0.14	0.49	0.546	1.015
0.16	0.486	0.549	1.01
0.18	0.481	0.552	1.006
0.20	0.476	0.556	1.001
0.22	0.4712	0.5588	0.9965
0.24	0.4662	0.562	0.9918
0.26	0.4615	0.5652	0.987
0.28	0.4566	0.5685	0.9823
0.30	0.4516	0.5717	0.9775
0.32	0.4467	0.5749	0.9727
0.34	0.4418	0.5781	0.9679
0.36	0.4368	0.5813	0.9631
0.38	0.4318	0.5845	0.9582
0.40	0.4268	0.5878	0.9533
0.42	0.4217	0.5909	0.9484
0.44	0.4166	0.5941	0.9435
0.46	0.4116	0.5973	0.9385
0.48	0.4064	0.6004	0.9335
0.50	0.4013	0.6036	0.9284
0.52	0.3961	0.6067	0.9233
0.54	0.391	0.6098	0.9182
0.56	0.3858	0.6128	0.9129
0.58	0.3804	0.6159	0.9078

0.60	0.3752	0.619	0.9025
0.62	0.3698	0.6219	0.8972
0.64	0.3645	0.6249	0.8918
0.66	0.3591	0.6278	0.8863
0.68	0.3537	0.6307	0.8808
0.70	0.3482	0.6335	0.8752
0.72	0.3427	0.6362	0.8695
0.74	0.3371	0.6389	0.8637
0.76	0.3316	0.6414	0.8579
0.78	0.3259	0.644	0.8517
0.8	0.3203	0.6464	0.8456
0.82	0.3145	0.6486	0.8393
0.84	0.3086	0.6506	0.8328
0.86	0.3028	0.6526	0.8262
0.88	0.2968	0.6543	0.8192
0.90	0.2408	0.6557	0.812
0.92	0.2847	0.6568	0.8045
0.94	0.2785	0.6575	0.7965
0.96	0.2722	0.6578	0.7881
0.98	0.2658	0.6574	0.7791
1.00	0.2592	0.6563	0.7694
1.02	0.2525	0.6543	0.7887
1.04	0.2456	0.6509	0.7467
1.06	0.2383	0.6457	0.7329
1.08	0.2308	0.6379	0.7167
1.1	0.2226	0.6263	0.6968
1.12	0.2135	0.6083	0.6711